

**UNCLASSIFIED**

---

---

**AD 297 218**

*Reproduced  
by the*

**ARMED SERVICES TECHNICAL INFORMATION AGENCY  
ARLINGTON HALL STATION  
ARLINGTON 12, VIRGINIA**



---

---

**UNCLASSIFIED**

NOTICE: When government or other drawings, specifications or other data are used for any purpose other than in connection with a definitely related government procurement operation, the U. S. Government thereby incurs no responsibility, nor any obligation whatsoever; and the fact that the Government may have formulated, furnished, or in any way supplied the said drawings, specifications, or other data is not to be regarded by implication or otherwise as in any manner licensing the holder or any other person or corporation, or conveying any rights or permission to manufacture, use or sell any patented invention that may in any way be related thereto.

18  
21  
22  
29  
97

297 218

63-2-5

TSFA  
TRANSPORTATION RESEARCH COMMAND  
FORT EUSTIS, VIRGINIA

CATALOGED  
AS AD NO

TCREC TECHNICAL REPORT 62-101

THE EFFECT OF THE VERTICAL POSITION  
OF THE CENTER OF GRAVITY ON THE STABILITY  
OF AN ANNULAR JET GROUND EFFECT MACHINE

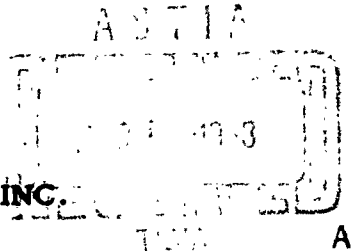
Task 9R99-01-005-02

Contract DA 44-177-TC-830

December 1962

prepared by:

NORMAN K. WALKER ASSOCIATES, INC.  
Bethesda, Maryland



DISCLAIMER NOTICE

When Government drawings, specifications, or other data are used for any purpose other than in connection with a definitely related Government procurement operation, the United States Government thereby incurs no responsibility nor any obligation whatsoever; and the fact that the Government may have formulated, furnished, or in any way supplied the said drawings, specifications, or other data is not to be regarded by implication or otherwise as in any manner licensing the holder or any other person or corporation, or conveying any rights or permission, to manufacture, use, or sell any patented invention that may in any way be related thereto.

\* \* \*

ASTIA AVAILABILITY NOTICE

Qualified requesters may obtain copies of this report from

Armed Services Technical Information Agency  
Arlington Hall Station  
Arlington 12, Virginia

\* \* \*

This report has been released to the Office of Technical Services, U. S. Department of Commerce, Washington 25, D.C., for sale to the general public.

\* \* \*

The information contained herein will not be used for advertising purposes.

\* \* \*

The findings and recommendations contained in this report are those of the contractor and do not necessarily reflect the views of the U. S. Army Mobility Command, the U. S. Army Materiel Command, or the Department of the Army.

HEADQUARTERS  
U. S. ARMY TRANSPORTATION RESEARCH COMMAND  
Fort Eustis, Virginia

The stability in roll of a typical annular jet GEM configuration has been investigated both experimentally and theoretically. It has been determined that, for the thin jet configuration, there are no stabilizing or destabilizing effects of a high center of gravity position on a hovering GEM completely free of the surface.

Theory predicts the existence of a stabilizing force as the configuration approaches the so-called "thick" jet or the plenum. Since the addition of trunks or skirts can result in a configuration which has the characteristics of a thick jet or plenum GEM, it is intended that further investigations of this effect will be conducted.

FOR THE COMMANDER:

  
KENNETH B. ABEL  
Captain, TC  
Adjutant



WILLIAM D. HINSHAW  
Project Engineer  
Ground Effect Research Group

Task 9R99-01-005-02  
Contract DA 44-177-TC-830  
TCREC Technical Report 62-101  
December 1962

THE EFFECT OF THE VERTICAL POSITION OF THE  
CENTER OF GRAVITY ON THE STABILITY OF AN  
ANNULAR JET GROUND EFFECT MACHINE

Prepared by  
Norman K. Walker Associates, Inc.  
Bethesda, Maryland

for  
U. S. ARMY TRANSPORTATION RESEARCH COMMAND  
FORT EUSTIS, VIRGINIA

## PREFACE

The work described in this report was performed by members of the staff of Norman K. Walker Associates, Incorporated, at their offices in Bethesda, Maryland, and their laboratory at Rockville, Maryland, during July, August and September 1962. Except as noted below, the experiments were devised by Mr. Norman K. Walker and Mr. Alastair Anthony, who also designed and constructed the test equipment and instrumentation, carried out the tests, prepared the illustrations and compiled this report.

The model GEM was built by the Hexicopter Model Research Company, Arvada, Colorado.

Mr. David A. Shaffer constructed the swinging trapeze, arranged the electrical circuits, and assisted with the recording of the data.

Mr. Lawrence C.J. Fricker contributed the theoretical analysis of Appendix I, and helped reduce the data into the form in which they appear in the report.

Mr. Harold Goldberg of Sommers Camera Exchange Inc., Washington, D.C., helped in the preparation of the 8mm. movie film, which was made during the course of the experiments, by kindly providing equipment and technical advice.

The Minneapolis-Honeywell "Visicorder" used to record the data is the property of U.S. Army, Office of the Surgeon-General.

## CONTENTS

	<u>Page</u>
PREFACE . . . . .	iii
CONTENTS . . . . .	v
LIST OF ILLUSTRATIONS . . . . .	vi
LIST OF SYMBOLS . . . . .	viii
SUMMARY . . . . .	1
INTRODUCTION. . . . .	2
SIMPLE THEORY . . . . .	4
MODEL AND EXPERIMENTAL PROCEDURE. . . . .	8
CONCLUSIONS . . . . .	35
REFERENCES. . . . .	36
 <b>APPENDIXES</b>	
I. Free GEM Equations. . . . .	37
II. Collected Data on the Rotation of the Resultant Force Vector with GEM Rotation. . . . .	46
DISTRIBUTION. . . . .	53

## ILLUSTRATIONS

<u>Figure</u>		<u>Page</u>
1	Roll Stability of a Displacement Craft. . . . .	3
2	Rolling GEM (No Damping). . . . . . . . . . .	4
3	Rolling GEM with Surface Contact. . . . . . .	7
4	The GEM Model - Sheet 1 . . . . . . . . . . .	9
	Sheet 2 . . . . . . . . . . .	10
	Sheet 3 . . . . . . . . . . .	11
5	Test Rig Set Up to Measure Lift or Static Stability . . . . . . . . . . .	13
6	GEM Model in 'trapeze' Rig Showing Intakes and Electrolytic Potentiometer. . . . . . .	14
7	GEM Test Rig Showing Optical System and Upper Pivot . . . . . . . . . . .	15
8	GEM Model - Quasi-free Oscillation Test . . .	16
9	Variation of Rise Height with Current for Fixed Lifts . . . . . . . . . . .	18
10	Variation of Lift with Rise Height for Fixed Motor Currents. . . . . . . . . . .	19
11	Static Stability in Roll. . . . . . . . . . .	21
12	Static Stability in Roll. . . . . . . . . . .	22
13	Static Stability in Roll. . . . . . . . . . .	22
14	Static Stability in Roll. . . . . . . . . . .	23
15	Variation of Static Stability with Height . .	24
16	Comparison of Measured Value of $\chi$ with Data from Appendix II . . . . . . . . . . .	27
17	Roll and Translational Oscillations . . . . .	30

## ILLUSTRATIONS (continued)

### LIST OF SYMBOLS

a	width of GEM
ap	displacement of lift vector from base center
b	length of GEM
d	diameter of circular GEM (Appendix II)
D	aerodynamic drag on GEM
F	water or obstacle resistance
G	jet width
G <sub>e</sub>	effective jet width = jet area per unit length of periphery
g	gravitational constant
h	rise height, height of base above ground
I	moment of inertia in roll about CG
i	motor current
L	lift force exerted by base
l	distance of trapeze pivot above GEM base
l <sub>D</sub>	distance of drag center above GEM base
l <sub>e</sub>	length of equivalent simple pendulum
l <sub>f</sub>	distance of sideforce center above base
l <sub>p</sub>	distance of free roll axis above base
l <sub>w</sub>	distance of CG above base
M	aerodynamic moment at base
M <sub>φ</sub>	= $\frac{\partial M}{\partial \phi} \cdot \frac{1}{L_a}$ , nondimensional roll stiffness
P	location of free roll axis

LIST OF SYMBOLS (continued)

Q location of obstacle or water resistance  
t jet width in plane of base  
W weight of GEM  
x distance sideways  
z distance vertically upwards  
 $\alpha$  angle of tilt (Appendix II)  
 $\delta$  angle of lift vector relative to normal to base (Appendix II)  
 $\zeta$  damping factor  
 $\lambda$  inward inclination of jet  
 $\phi$  angle of tilt of GEM  
 $x_\phi$   $\frac{\partial x}{\partial \phi}$   
x angle of lift vector with normal to base  
 $\omega$  angular frequency of oscillation

## SUMMARY

Measurements were made on an electrically powered annular thin jet Ground Effect Machine in hovering flight to determine the lift versus height at various power levels; the restoring moment and sideforce due to the angle relative to the ground; the roll stability with the machine pivoted at the base, and then at intermediate and high positions above the base, with the center of gravity low, high and extra high for each pivot position; and the behavior of the machine with the pivot free to move sideways. Finally the machine was flown without any constraints in the low, high and extra high CG positions.

It was determined that the lift vector remains normal to the base within an angle not greater than 0.06 times the angle between the machine and the ground, and that the stability is virtually unaffected by the height of the CG relative to the base, provided that the machine is clear of contact with the ground or any other obstacle.

The experiments are illustrated by 16 diagrams and 4 photographs. An 8mm. color movie was made showing each of the tests in the order in which they were performed.

## 1. INTRODUCTION

In most surface transport vehicles it is necessary to limit the height of the center of gravity in order to preserve a margin of safety against overturning following a small or finite angular displacement in roll. This is generally because the reactions of the supporting system include a vertical force opposing the weight but displaced by an amount proportional to the height and the angle of tilt. This exerts an overturning moment which will prevail over the restoring forces if the height is large enough. Figure 1.

The GEM is peculiar in that the main lift is due to static air pressure under the base which to a first approximation continues to act normal to the base when the machine is tilted, and therefore does not exert an overturning moment about the CG, whatever the height may be. We may therefore expect the rolling stability to be independent of the height of the CG, and presume that instability cannot be caused by variation in CG height.

However, Stanton-Jones on page 44 of reference 1 gives an expression for the static stability which does involve the height of the CG above the flat bottom of the machine although in Figures 15 and 17 of the same paper he shows the resultant lift as normal to the base of the GEM and in subsequent correspondence insisted that a CG height correction was in fact necessary for satisfactory behavior.

In order to try to establish experimentally the true facts of the matter the present investigation was authorized by U. S. Army Transportation Research Command under Contract Number DA 44-177-TC-830.

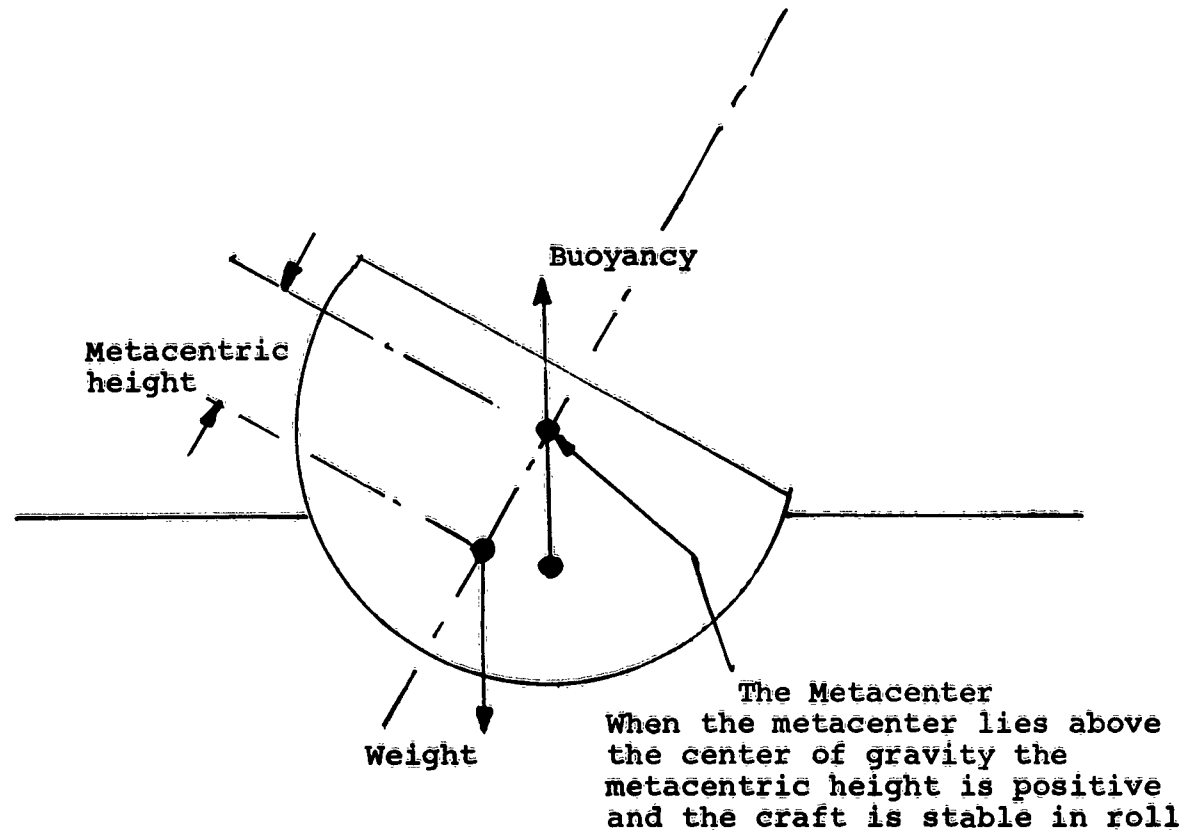


Figure 1. Roll Stability of a Displacement Craft

## 2. SIMPLE THEORY

### 2.1 No Contact with the Surface

Some insight into the roll behavior of a GEM may be gained by assuming that damping of all oscillations is small, and that the terms causing damping can be neglected in the analysis.

Consider the GEM shown in Figure 2. The GEM is rolled to an angle  $\phi$ , and the resultant force  $L$  is rotated through an angle  $\phi + x$  to the vertical. A moment  $M$  determined by the angle  $\phi$  is generated by the roll, and there will, of course, be a lateral force  $L(\phi + x)$ , assuming that the angles are small.

It is assumed that the rolling moment due to rolling velocity and the lateral force due to lateral velocity can both be neglected.

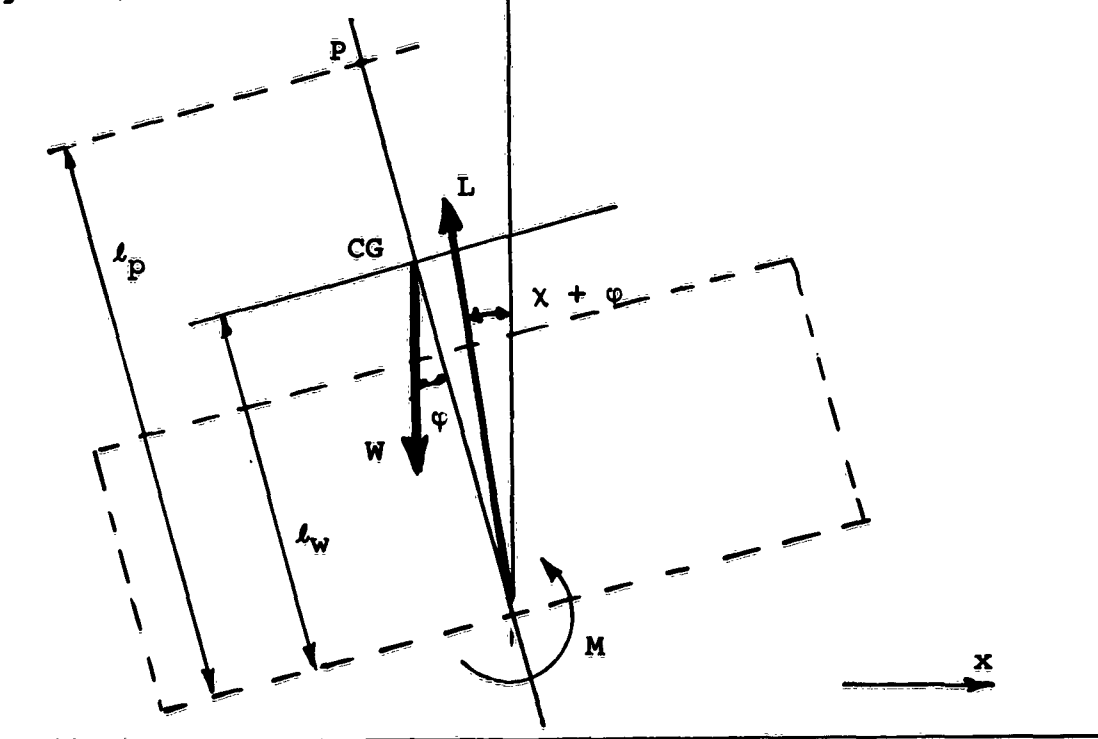


Figure 2. Rolling GEM with no Damping Forces

Taking moments about the CG,

$$I\ddot{\varphi} = \frac{\partial M}{\partial \varphi} \cdot \varphi - L\ell_w \frac{\partial x}{\partial \varphi} \cdot \varphi$$

which represents an undamped oscillation of frequency

$$\left[ \frac{1}{I} \frac{\partial}{\partial \varphi} (-M + L\ell_w x) \right]^{\frac{1}{2}}$$

and period

$$\frac{2\pi}{\left[ \frac{1}{I} \frac{\partial}{\partial \varphi} (-M + L\ell_w x) \right]^{\frac{1}{2}}}$$

The lateral oscillation is forced by the roll so that

$$\ddot{x} + g\varphi \left( \frac{\partial x}{\partial \varphi} + 1 \right) = 0$$

and this represents a lateral oscillation of CG forced by the roll amplitude, with the displacement  $x$  in phase with  $\varphi$  since no restoring force proportional to  $x$  or  $\dot{x}$  is assumed to exist.

The combined mode will therefore be an oscillation in roll about the CG, combined with a lateral oscillation of the CG in the same direction as the movement of the base due to the roll.

At some point P at a distance  $\ell_p - \ell_w$  above the CG the lateral acceleration will be zero.

$$\therefore (\ell_p - \ell_w) \ddot{\varphi} = \ddot{x}$$
$$\ell_p - \ell_w = \frac{g \left( \frac{\partial x}{\partial \varphi} + 1 \right)}{\frac{1}{I} \frac{\partial}{\partial \varphi} (-M + L\ell_w x)}$$

Writing  $x = x_\varphi \varphi$ , note that if  $x_\varphi$  is constant, the distance  $\ell_p - \ell_w$  is equal to  $(1 + x_\varphi)$  times the length of a simple pendulum of the same period as the oscillation.

In the particular case of the thin jet GEM it is believed that  $x_\phi = 0$ ; therefore  $x$  is always zero and the GEM will oscillate about an axis stationary in space located above the CG of the machine, the distance from this axis to the CG being the same as the length of a simple pendulum of the same period.

## 2.2 The Effect of Contact with the Surface

Suppose that some part of the GEM touches the surface, so that lateral movement is impeded. Such a condition can arise if the edge strikes the ground, or if the machine is fitted with a keel which dips slightly below the surface of the water.

The solution in the latter case is complex - see Appendix I - since a lateral force proportional to velocity will be generated.

However, if we assume the effect is very large, the result will be that lateral motion of the machine at this point will be prevented, and the machine will rotate in roll about the point of contact. (Q)

Hence the stability of the GEM will depend on the condition that the total moment about the point Q must be stabilizing. Figure 3.

The condition cited by Stanton-Jones, reference 1, may be intended to guard against instability when the bottom of the GEM touches the crest of a wave.

## 2.3 Experimental Confirmation

To support the assertions of sub-sections 2.1 and 2.2, some further evidence is needed. It was therefore proposed:

- a. To expound a more comprehensive theory including damping effects in roll and translation.
- b. To measure the static stability derivatives for a model.
- c. To check the behavior of the model in free or partly constrained flight to verify the relation between the CG and the rolling axis position, and the effect of surface contact.

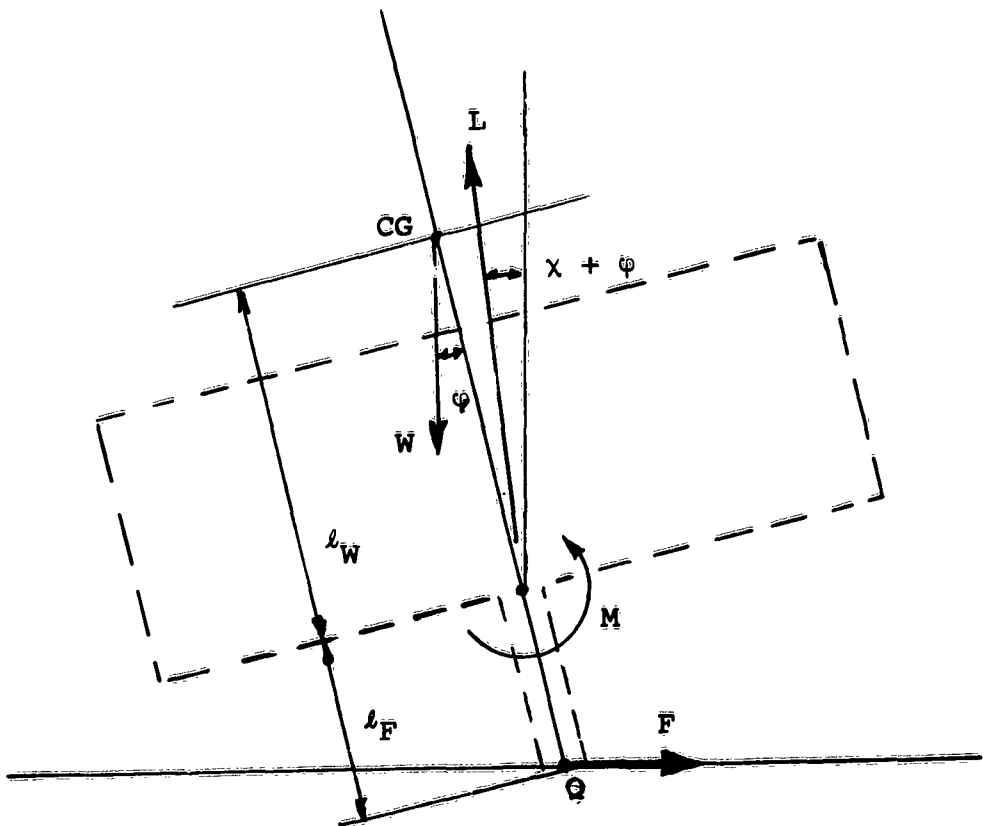


Figure 3. Rolling GEM with Surface Contact

### 3. MODEL AND EXPERIMENTAL PROCEDURE

#### 3.1 The Model GEM

Early experiments in 1961 with a free flight plenum chamber model suggested that the simple theory outlined in Section 2 explained the main features of the motion, so it was agreed under this contract to build a 'thin' annular jet model with more accurately defined characteristics.

The model shown in Figure 4 was built to our requirements by the HEXICOPTER Model Research Company of Arvada, Colorado. On arrival it was fitted with a frame and rigging to support ballast weights in a high position, or on lateral booms to give roughly the same moment of inertia. In the lower position the CG is 34.1% of the beam above the base, and in the higher position is 65.8% above the base. The bare model weighs 224.6 grams, and the two CG trim weights are 32 grams apiece. For details see Table 1.

The model is powered by two small permanent magnet direct current motors connected in series to ensure that the same current flows to both motors. The fans are mounted in faired entries, but no special provision is made to distribute the air evenly to the periphery. The annular jet is vertical and 1/8" wide.

Stabilizing jets each 1/8" wide are cut in the base, the total area of the stabilizing jets being 50% of the area of the annular jet. They give excellent stability.

The original intention was to build an ellipsoidal bowl for free flight tests, the stability derivatives being determined from the motion and attitude in the bowl, but preliminary experiments showed that this procedure was insufficiently accurate to check the theory.

A special test rig was built which enabled the model to pivot freely about the roll and one other axis, while restraining it in yaw and fore-and-aft motion. Figures 5, 6, 7, and 8.

#### 3.2 Measurement of lift

The model was pivoted slightly above the CG between the arms of a horizontal weigh beam, and the beam was pivoted to allow vertical movement of the model. The movement was magnified

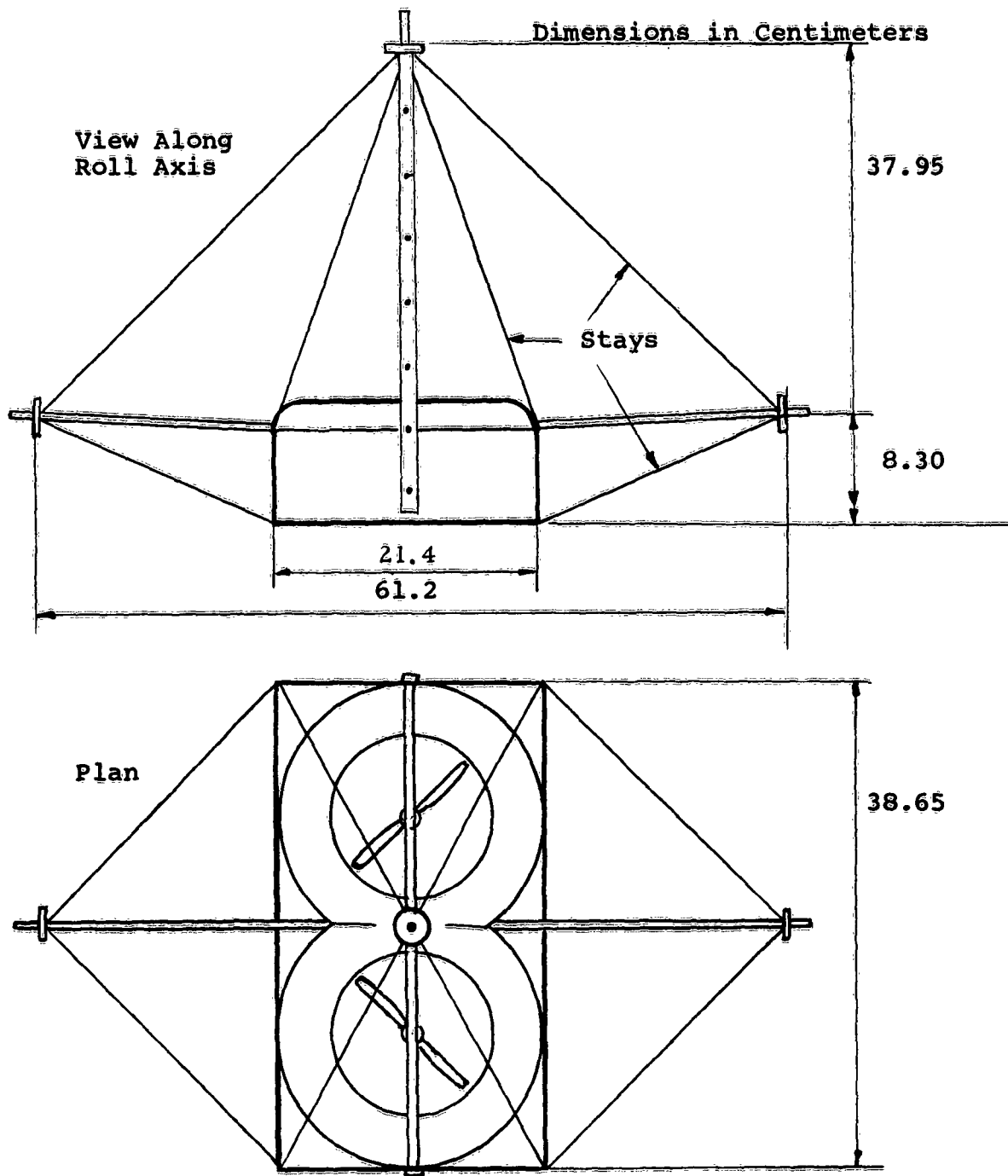
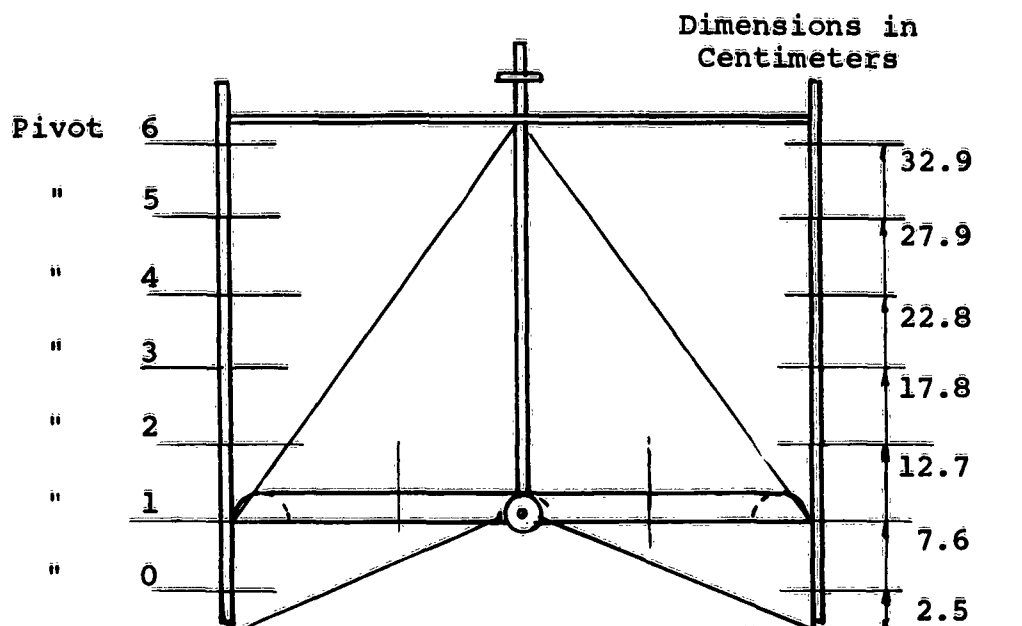


Figure 4 - Sheet 1. The GEM Model



Side View

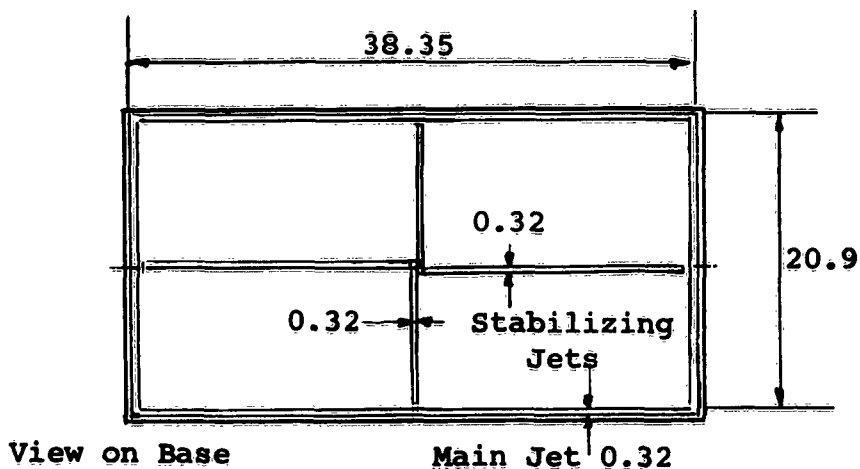
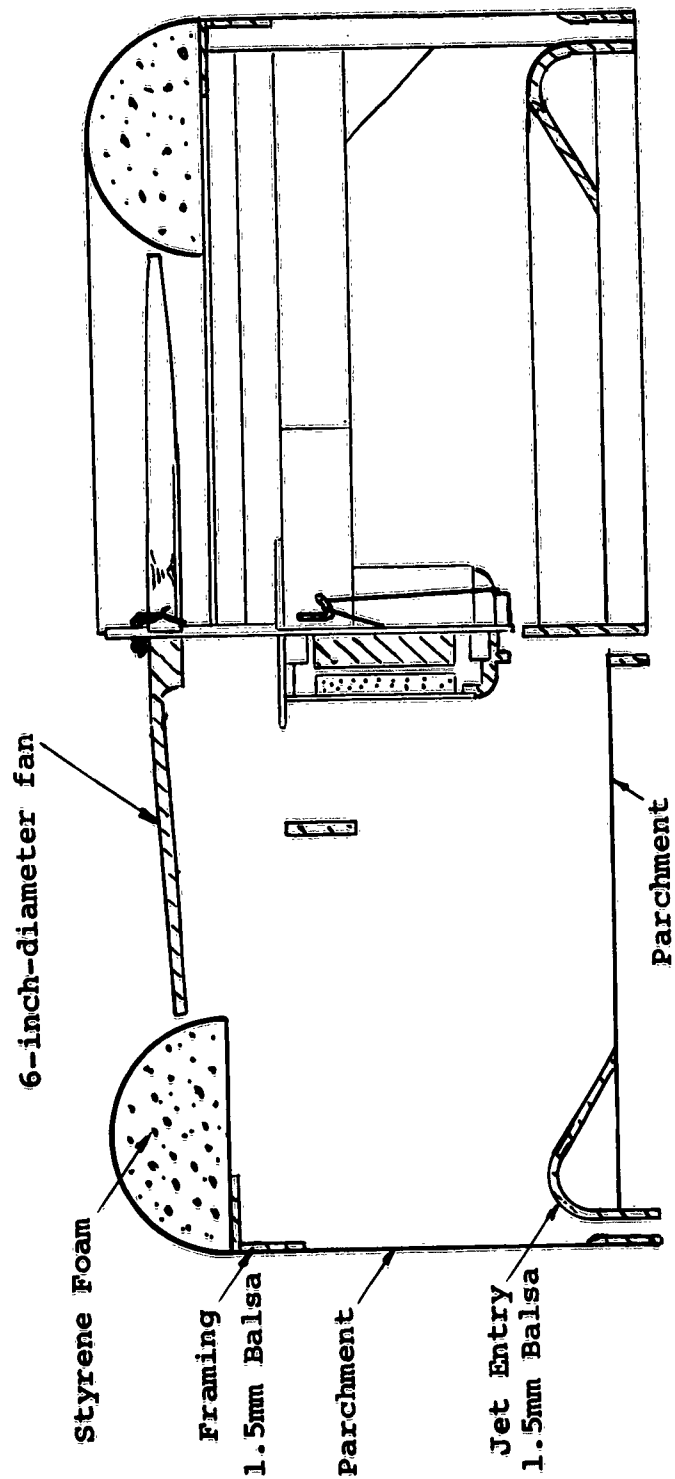


Figure 4 - Sheet 2. The GEM Model



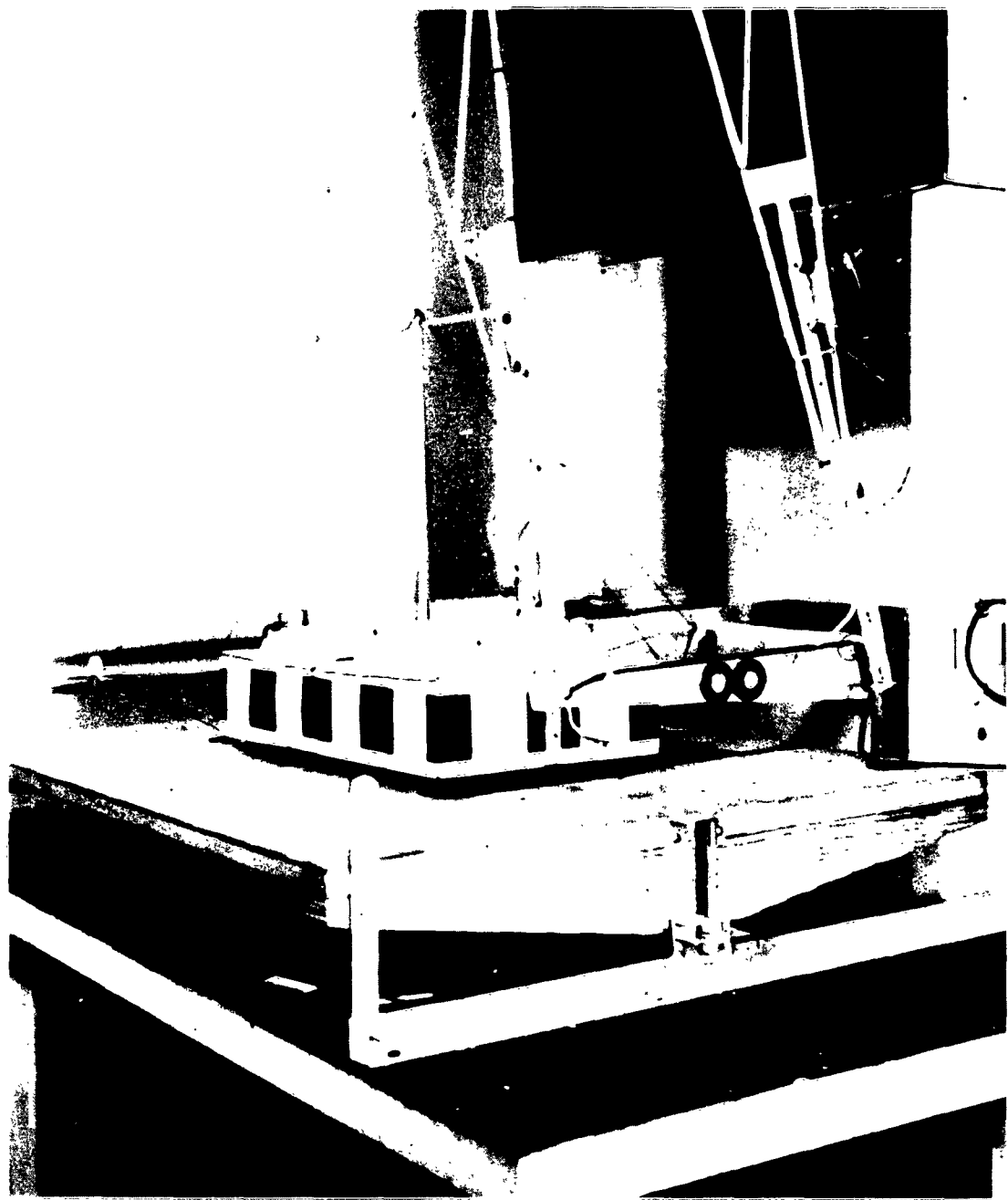
Transverse  $\frac{1}{2}$  Section and Interior View of Motor Mounting

Figure 4 - Sheet 3. The GEM Model

TABLE 1  
DETAILS OF MODEL

	NO Weights	Low CG	High CG	Very High CG
Weight of GEM ("W" in grams)	224.6	288.6	288.6	-
Original fans	221.0	284.0	284.0	389.5
Improved low pitch fans*				
Moment of Inertia about CG ("I" in gm cm <sup>2</sup> )	17,000.0	76,600.0	66,230.0	120,230.0
Height of CG above base (L <sub>w</sub> in cm)	6.8	7.12	13.75	22.35
Standard Test Altitude (h = L <sub>f</sub> in cm)	0.66	0.66	0.66	0.66
Beam of GEM (to outer edge of jet) (a in cm)	20.9	20.9	20.9	20.9
Length of GEM (to outer edge of jet) (b in cm)	38.35	38.35	38.35	38.35
Base area cm <sup>2</sup>	802.0	802.0	802.0	802.0
Jet width cm	0.32	0.32	0.32	0.32
Stabilizing jet width cm	0.32	0.32	0.32	0.32

\*Used only in last series of tests, including free flight.



**Figure 5. Test Rig Set Up to Measure Lift or Static Stability**

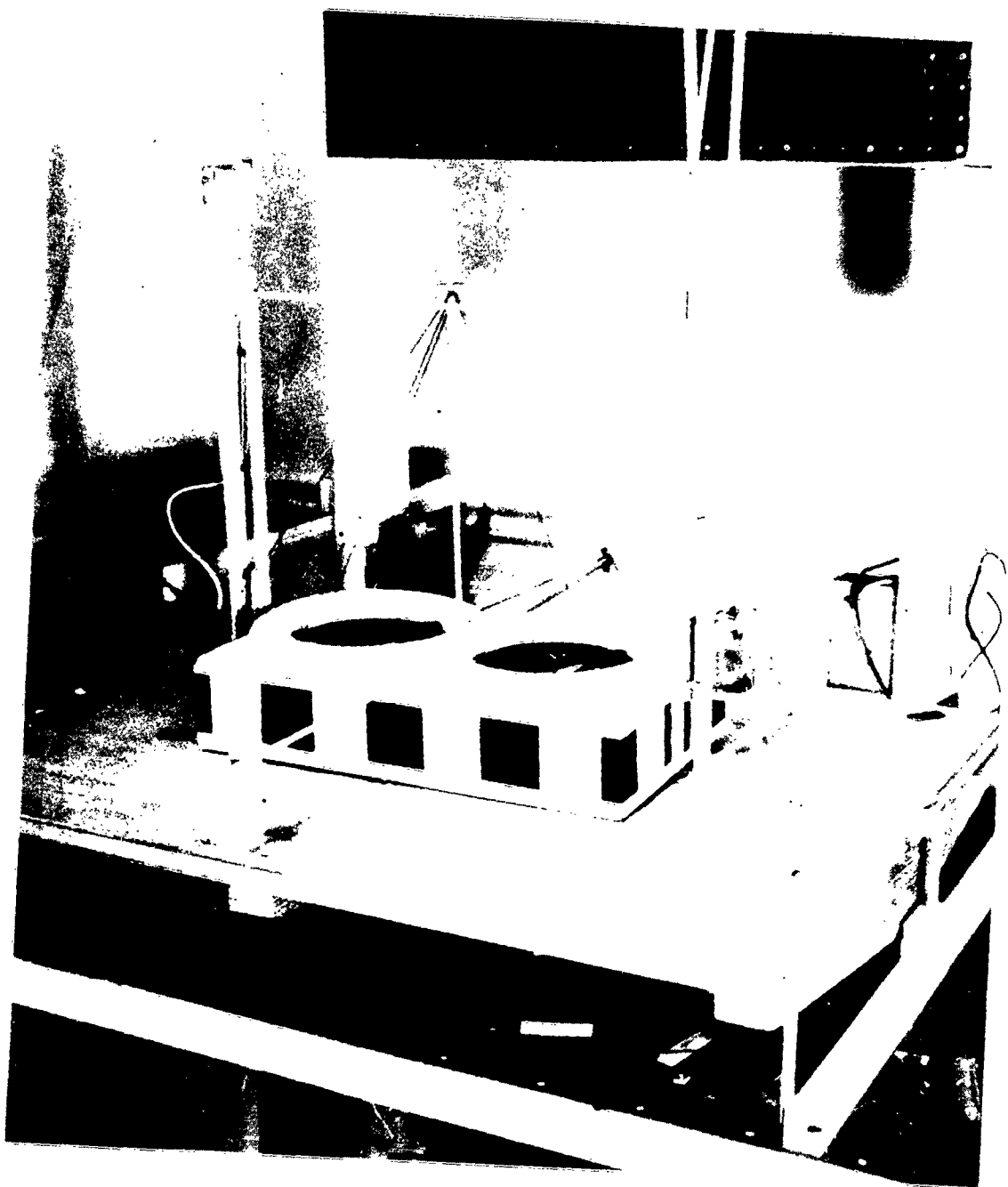
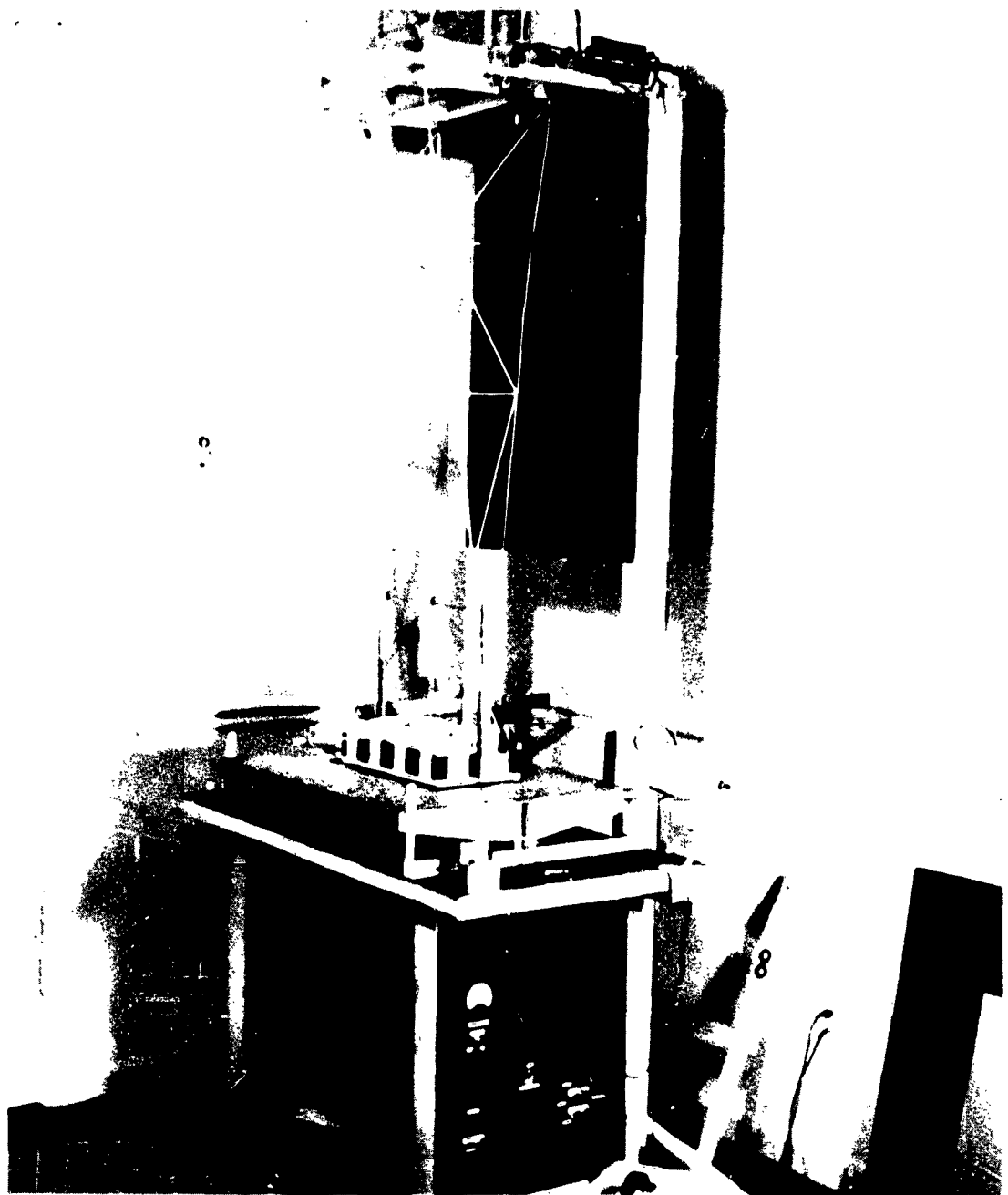


Figure 6. GEM Model in 'Trapeze' Rig Showing Intakes and Electrolytic Potentiometer



**Figure 7. GEM Test Rig Showing Optical System and Upper Pivot**



**Figure 8. GEM Model - Quasi-Free Oscillation Test**

by an optical lever system so that vertical displacements were read out direct on an enlarged scale. The pivoting of the model near the CG ensured that the inherent stability would hold the model parallel to the ground board.

Readings were then taken of the variation of rise height with current for the model alone lifting its own weight, and then with weight increased or decreased by adding weights to either end of the weigh beam. Figure 9.

These were then cross-plotted to give the variation of lift with rise height for suitable fixed current values. Figure 10.

The variation of lift with current is of strange form, no doubt reflecting the variation of fan and duct efficiencies with fan speed, but the results are remarkably consistent and the cross plots of rise height against  $(lift)^{-3/2}$  are linear, as would be expected.

From the graphs the lift of the GEM can be read for any rise height and motor current.

See also the tabulated results in Table 2.

### 3.3 Measurement of static stability in roll

The lift balance beam was now clamped to give a fixed rise height. An additional mirror was fixed to the GEM model to give a reading of roll angle.

The variation of roll angle with applied rolling moment (obtained by hanging known weights on the yardarms of the GEM) was recorded for a given motor current, and is plotted in the form of  $M/L_a$  versus  $\varphi$  (radians) in Figure 11 for a motor current of 1.2 amps and a rise height of 0.7 cm. ( $h/a = 0.0335$ .)

As a check a second run was made at this altitude with a motor current of 1.0 amp and showed excellent agreement with the previous results.

Further tests were made at  $h/a$  values of 0.0174, 0.080 and 0.114, and also appear consistent. (The large zero error for  $h/a = 0.114$  is not significant since the model was not statically balanced and the roll stability was very low at this height.) Figures 12, 13, and 14.

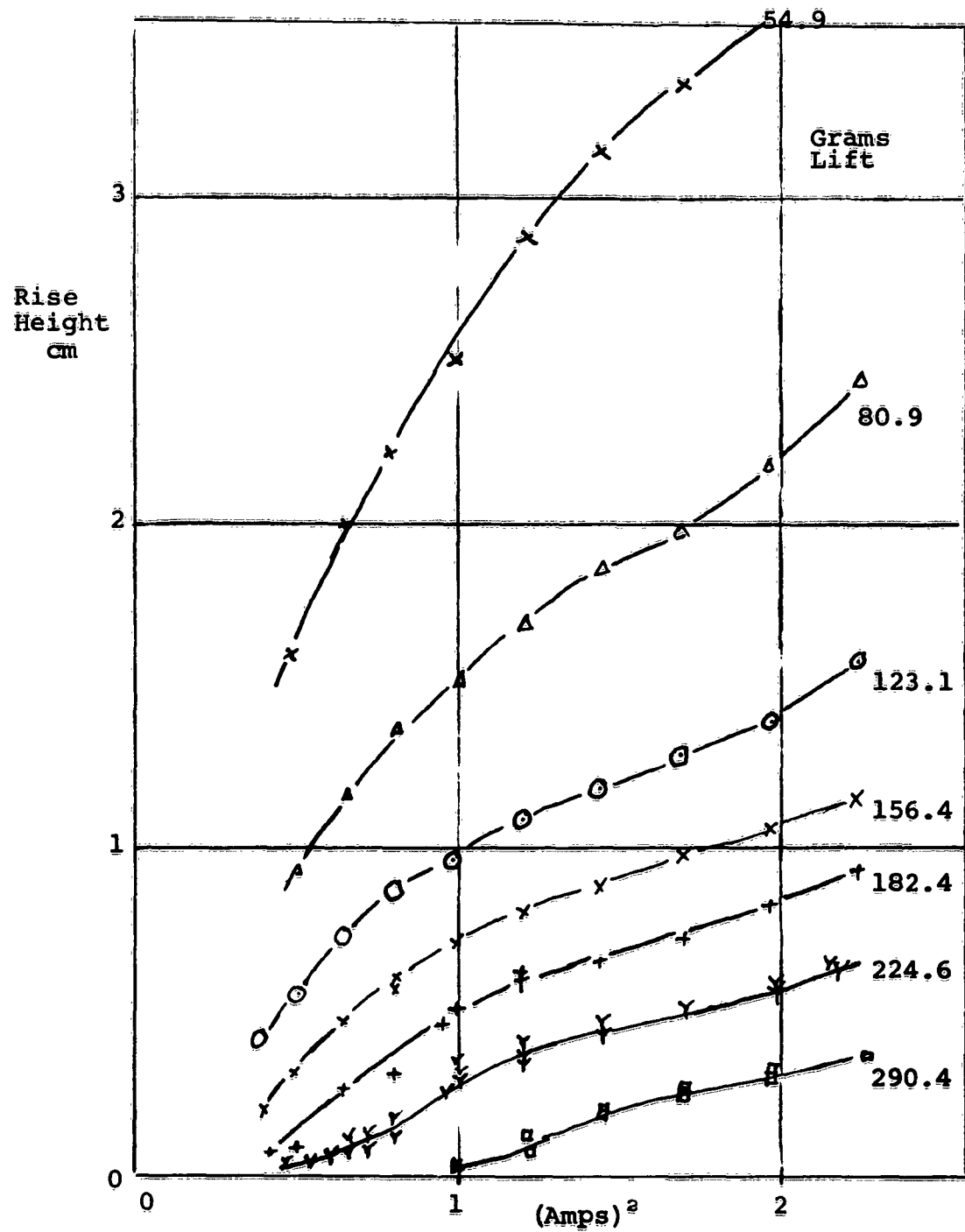


Figure 9. Variation of Rise Height With Current for Fixed Lifts

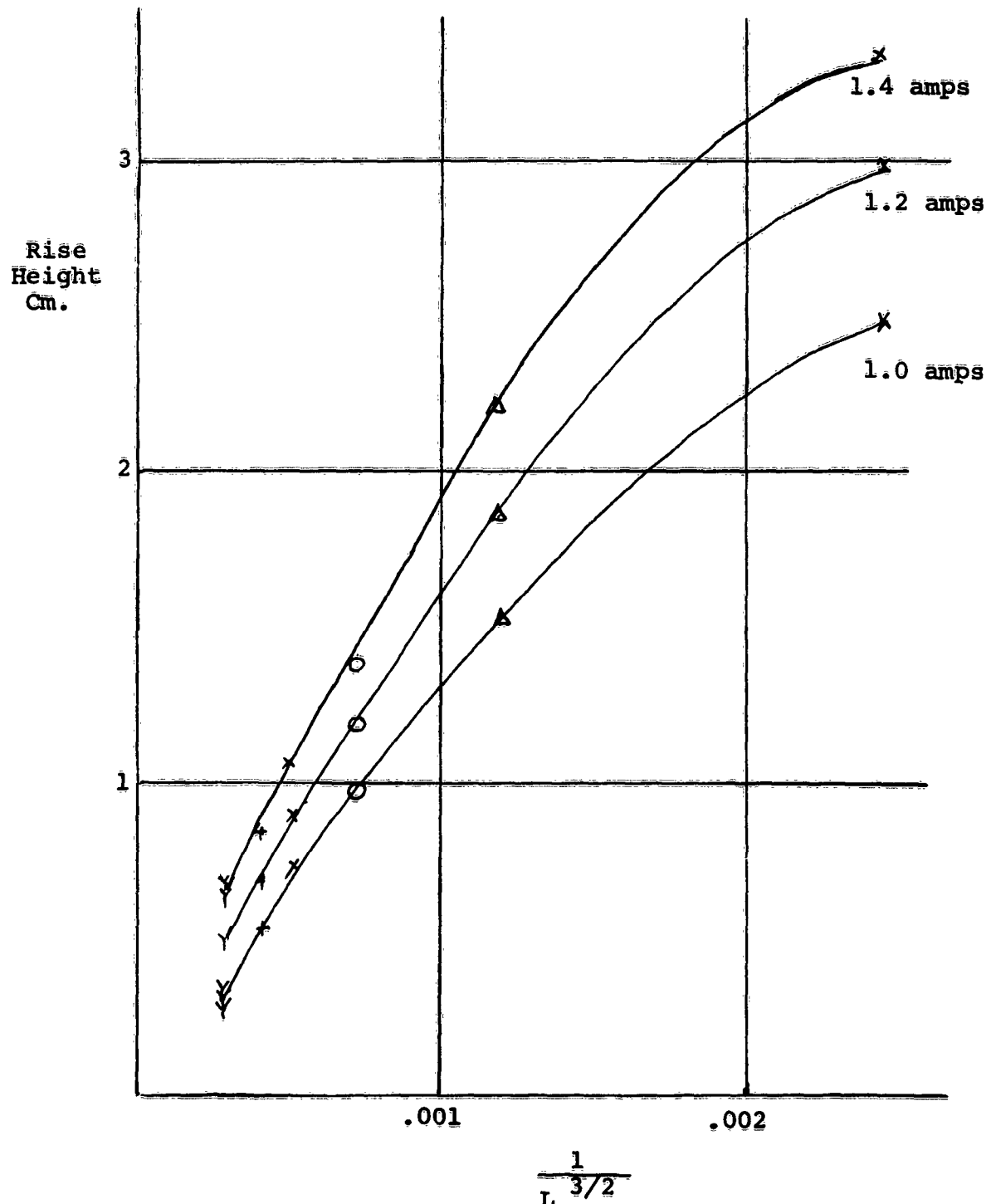


Figure 10. Variation of Lift with Rise Height for Fixed Motor Currents

TABLE 2  
VARIATION OF RISE HEIGHT WITH CURRENT FOR FIXED LIFTS

LIFT (grams)	i (amps)						
	h (cm)						
290.4	i	1.50	1.40	1.40	1.30	1.30	1.20
	h	0.377	0.338	0.325	0.260	0.273	0.234
224.6	i	1.20	1.10	1.10	1.00		
	h	0.221	0.091	0.117	0.039		
182.4	i	1.47	1.46	1.40	1.40	1.30	1.30
	h	0.610	0.622	0.584	0.590	0.503	0.503
156.4	i	1.20	1.20	1.10	1.10	1.10	1.10
	h	0.480	0.468	0.376	0.364	0.402	0.337
123.1	i	1.10	1.00	0.97	0.90	0.90	0.90
	h	0.286	0.298	0.247	0.182	0.143	0.143
123.1	i	0.85	0.85	0.80	0.80	0.80	0.75
	h	0.078	0.072	0.065	0.065	0.051	0.051
123.1	i	0.75	0.71	0.70	0.70	0.69	0.65
	h	0.039	0.039	0.051	0.013	0.039	0.013
123.1	i	1.50	1.40	1.30	1.20	1.10	1.10
	h	0.950	0.845	0.740	0.675	0.610	0.625
123.1	i	1.0	0.97	0.90	0.80	0.70	0.65
	h	0.503	0.494	0.338	0.286	0.078	0.065
123.1	i	1.50	1.40	1.30	1.20	1.10	1.00
	h	1.170	1.078	0.987	0.890	0.818	0.727
123.1	i	0.90	0.90	0.80	0.70	0.64	
	h	0.620	0.610	0.480	0.324	0.207	
123.1	i	1.50	1.40	1.30	1.20	1.10	1.00
	h	1.590	1.400	1.290	1.190	1.100	0.975
123.1	i	0.90	0.80	0.70	0.63		
	h	0.880	0.740	0.560	0.429		

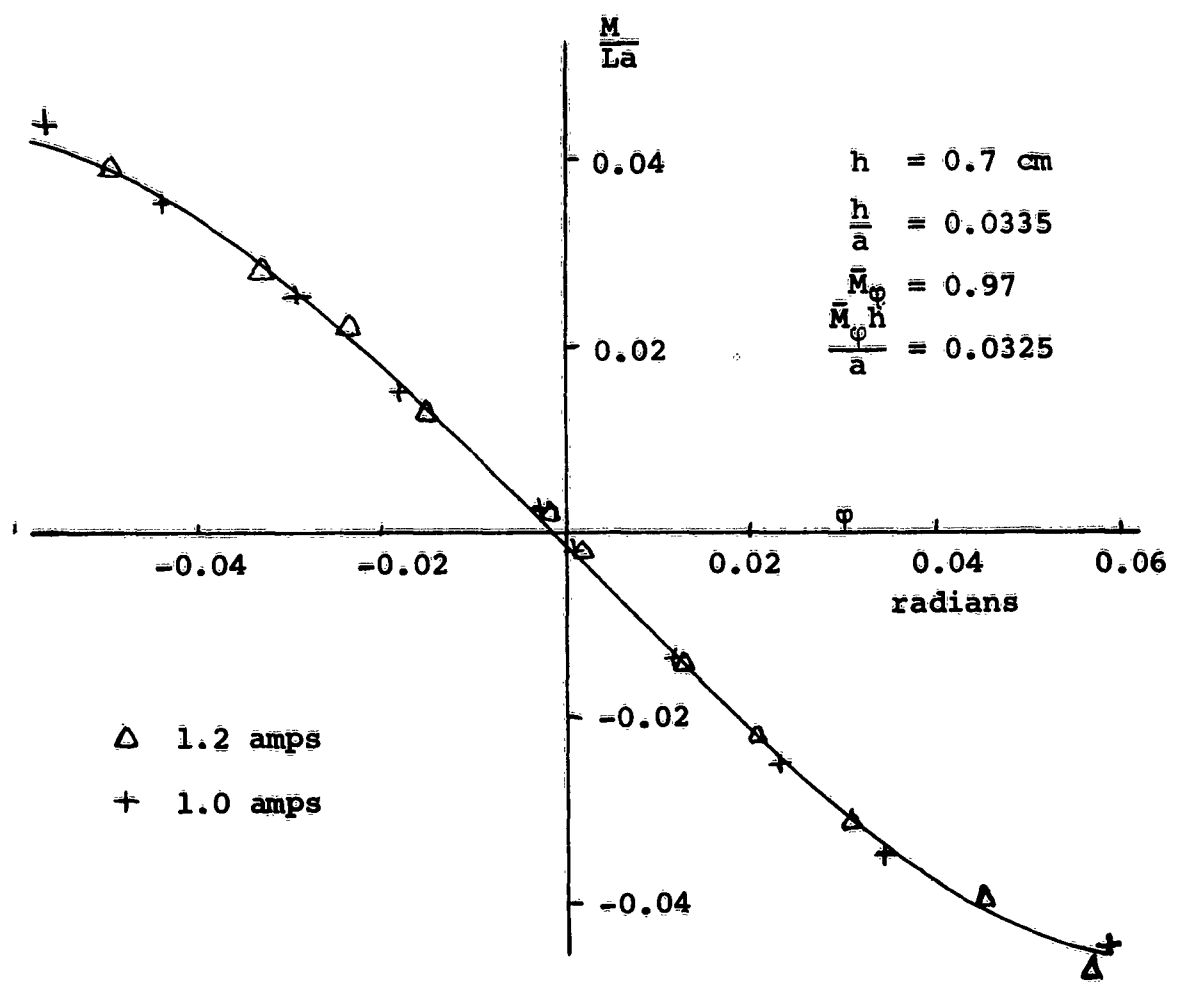


Figure 11. Static stability in Roll

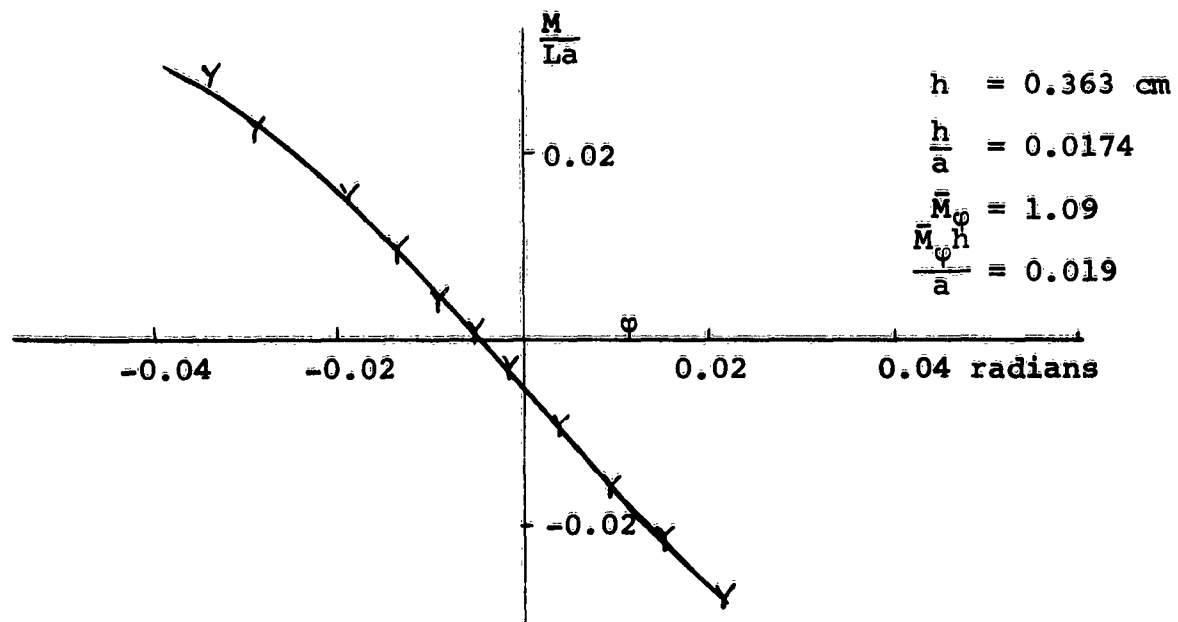


Figure 12. Static Stability in Roll

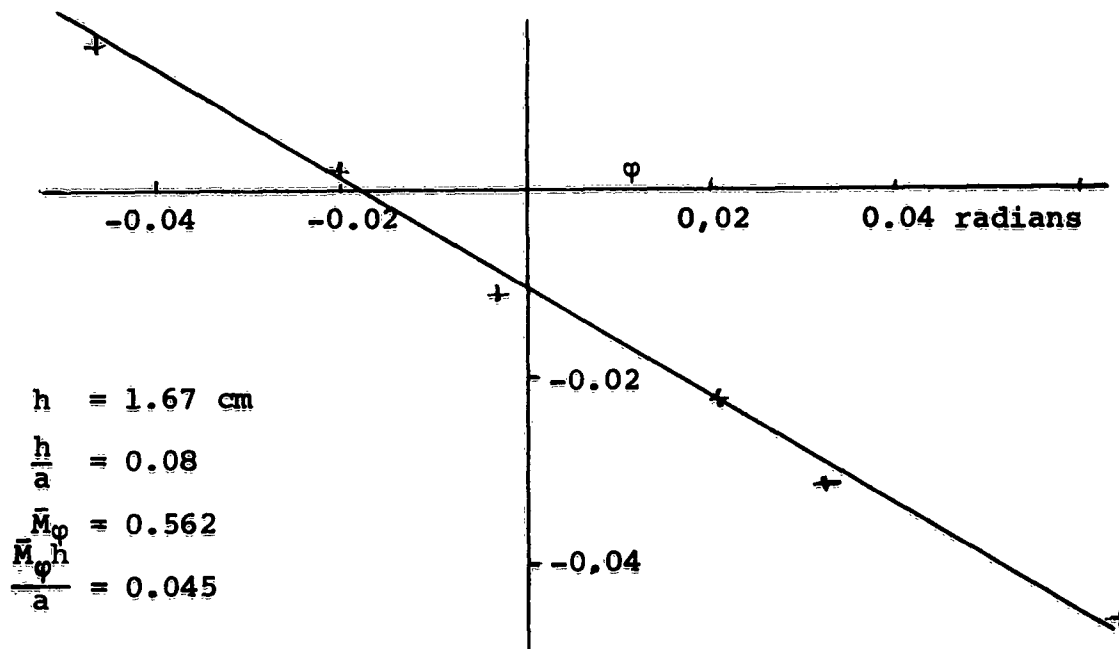


Figure 13. Static Stability in Roll

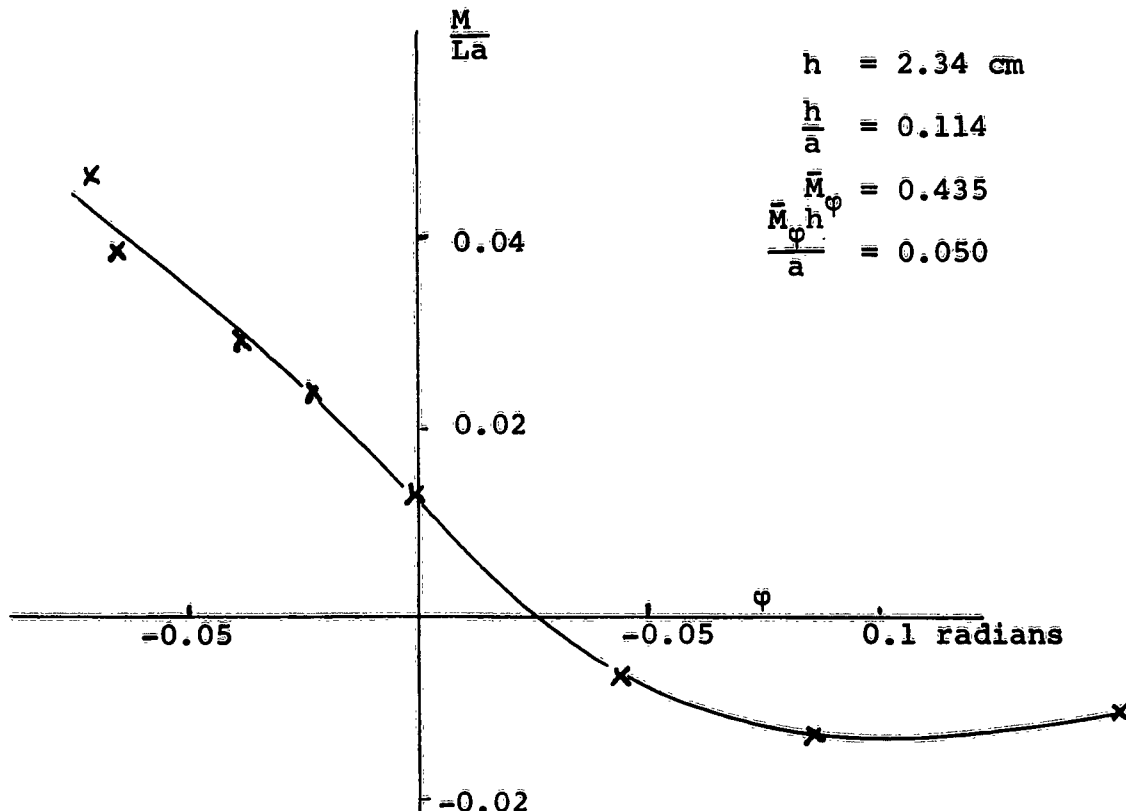


Figure 14. Static Stability in Roll

The slope at zero roll angle was read off from the curves, multiplied by  $h/a$ , and plotted against  $h/G$ , the height/thickness ratio of the jet in Figure 15. M.C. Eames, in reference 2, has determined the maximum static stability to be expected from a GEM in which the two halves of the air cushion defined by the roll axis are separated by a flexible pressure-supporting membrane. His result for the case where the two halves of the annular jet are supplied from a single source of constant total head - the plenum box in our case - is also plotted in Figure 15; also his own suggestion of the practical maximum (50%) where the membrane is replaced by a large transverse jet.

The results indicate that at all altitudes the stabilizing jets give about 90% of the practical maximum.

Detailed results are given in Table 3.

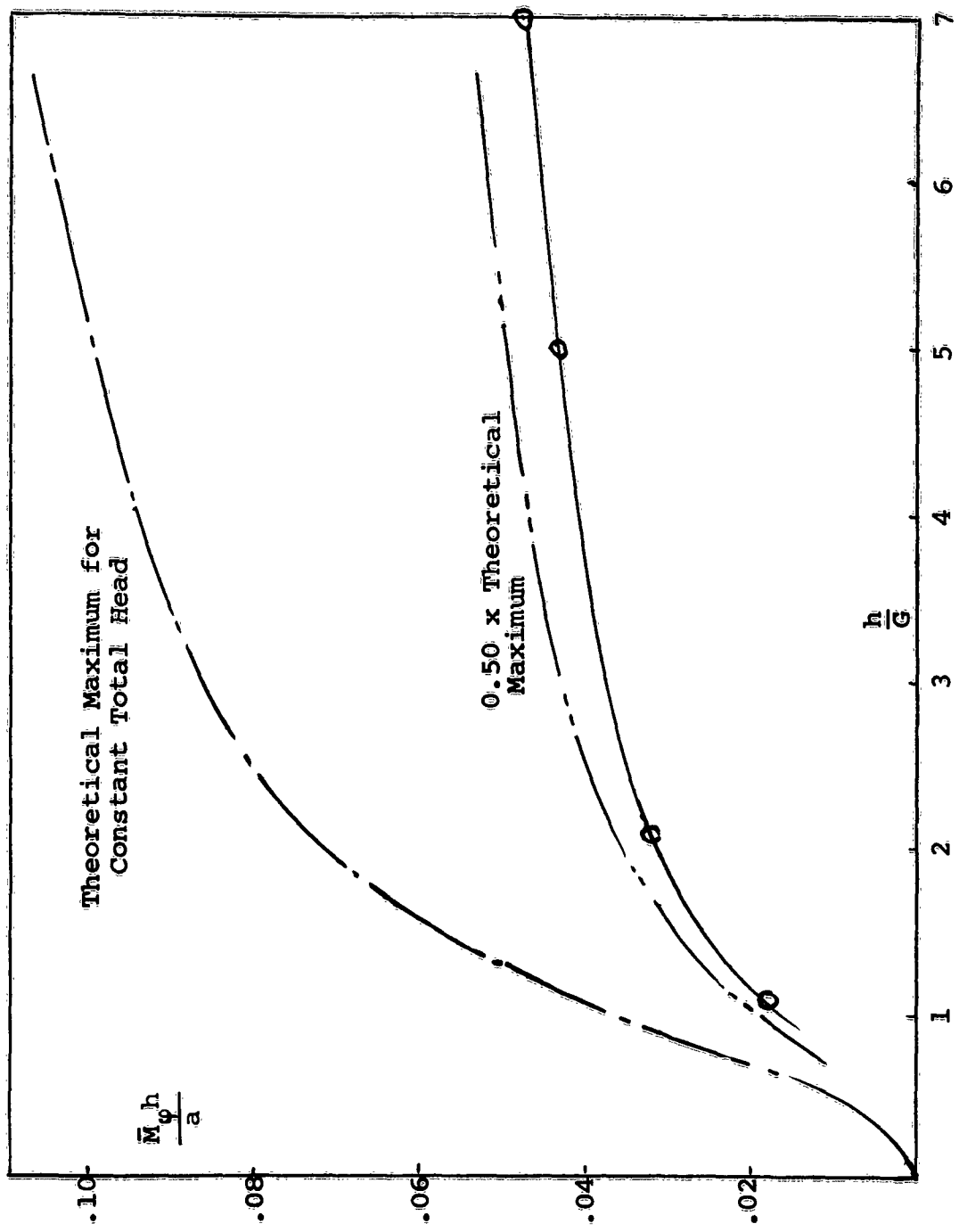


Figure 15. Variation of Static Stability with Height

TABLE 3  
STATIC STABILITY IN ROLL

$h/a = 0.0174$	$i = 1.2 \text{ amp}$	Lift	$M/La$	$\Phi$	0	-0.0035	-0.0095	-0.016	-0.022	-0.028
243					-0.0005	-0.0015	0.00425	0.009	0.0155	0.021
			$M/La$	$\Phi$	0	0.0040	0.0100	0.0160	0.2225	0.0285
			gm wt.		-0.00050	-0.0090	-0.0140	-0.0190	-0.0265	-0.0335
$h/a = 0.0335$	$i = 1.2 \text{ amp}$	Lift	$M/La$	$\Phi$	-0.00051	-0.0134	-0.0220	-0.0310	-0.0390	-0.0470
181					0.00055	0.131	0.0212	0.0314	0.0454	0.0518
			$M/La$	$\Phi$	0.00053	0.0131	0.0220	0.028	0.0390	
			gm wt.		-0.00051	-0.0150	-0.0234	-0.0326	-0.0495	
$h/a = 0.0335$	$i = 1.0 \text{ amp}$	Lift	$M/La$	$\Phi$	0	0.0055	-0.0140	-0.0250	-0.0350	-0.0440
159					-0.0030	0.0037	0.0135	0.0240	0.0345	0.0590
			$M/La$	$\Phi$	0.0055	0.0150	0.0250	0.0350	0.0440	
			gm wt.		-0.0081	-0.0183	-0.0293	-0.0430	-0.0560	
$h/a = 0.080$	$i = 1.2 \text{ amp}$	Lift	$M/La$	$\Phi$	-0.0020	-0.0107	-0.0235	-0.0320	-0.0460	0.0155
88.5					-0.0219	-0.0030	0.0210	0.0320	0.0645	0.0465
			$M/La$	$\Phi$	0	0.0020	0.0130	0.0240	0.0290	0.0390
			gm wt.		-0.0220	0.0	0.0215	0.0380	0.0625	0.0710
$h/a = 0.114$	$i = 1.2 \text{ amp}$	Lift	$M/La$	$\Phi$	0.0030	0.0130	0.0240	0.0290	0.0390	0.0467
56.4					-0.0067	-0.0131	-0.0109			
			$M/La$	$\Phi$	-0.0440	-0.0850	-0.1260			
			gm wt.							

### 3.4 Measurement of Resultant Force Rotation Due to Roll Angle

The measurement of the side force due to roll angle is very delicate since it must be made in the presence of a large lift.

For this measurement the model was supported from a long, balanced "trapeze" structure pivoted to rotate about an axis 147.3 centimeters above ground board. The model was accurately leveled and then clamped in the trapeze. Displacement of the model and trapeze could then be read by another mirror system.

The model was given an equivalent roll angle by tilting the ground board, the tilt also being measured by an optical pointer. The tilt produced a slight displacement of the model away from the ground board, and this was nulled by adding small known weight to the yardarm of the GEM.

The applied moments and ground board tilt were recorded.

These moments as measured are represented by the expression

$$(M_\phi - L\ell x_\phi) \phi$$

where  $\ell$  is the height of the trapeze pivots above the GEM base ( $= 146.6\text{cm}$ ).

$M$  was determined by the measurement of roll stability, section 3.3. Subtracting this in the appropriate sense we obtain values for the term  $L\ell x_\phi$ .  $L$  is known from the motor current versus lift calibration of section 3.2.

Hence values for  $x_\phi$  are determined, and are seen to be very small, lying between minus 0.06 and zero.

Measured points are plotted in Figure 16 and are compared with results derived from the University of Wichita and other tunnel tests in Appendix 2. It is evident that the special procedure and equipment used is far more accurate than the use of a general purpose six-component wind tunnel balance, and that for the GEM tested the resultant force is substantially normal to the base.

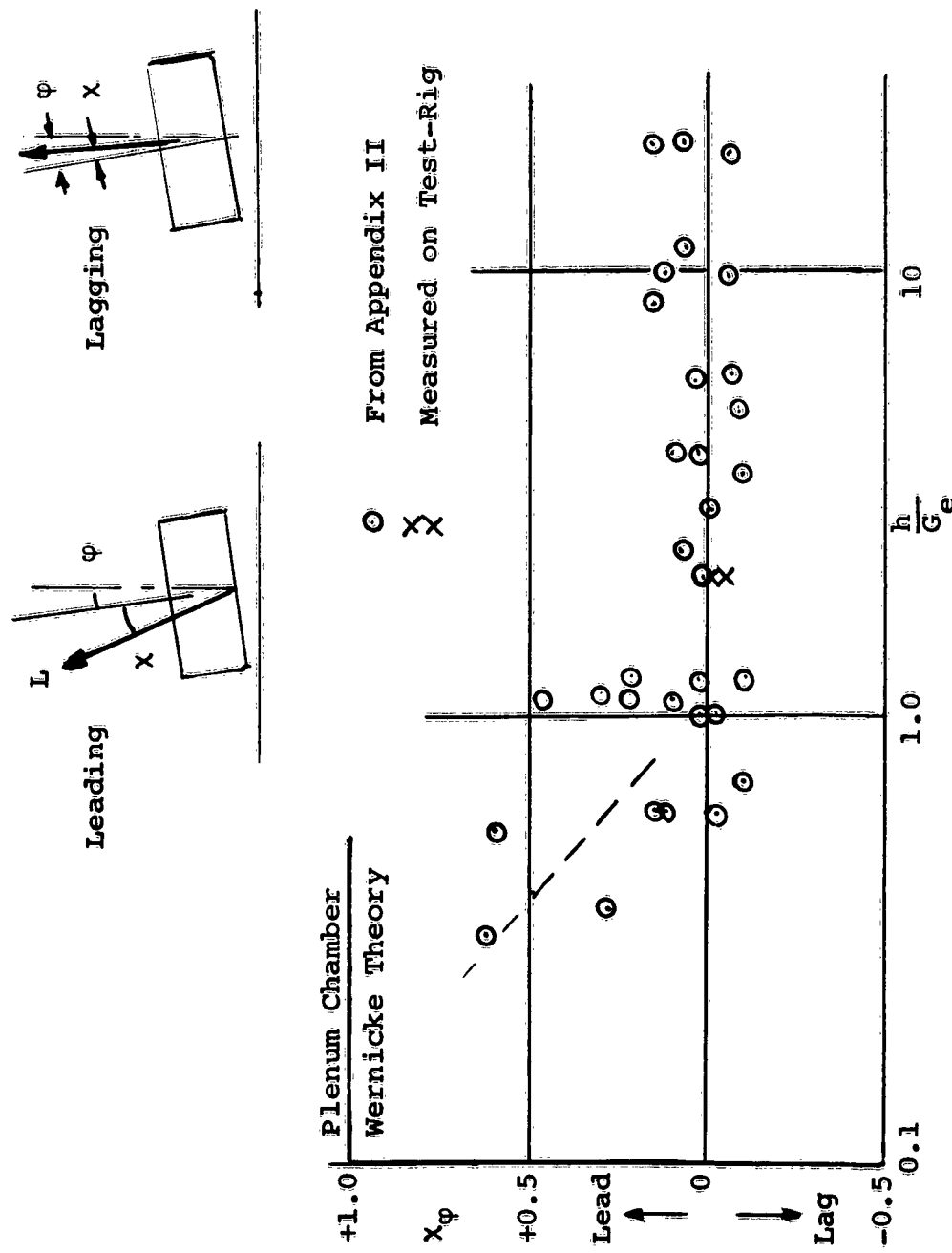


Figure 16. Comparison of Measured Value of  $x_\varphi$  with Data from Appendix II

### 3.5 Quasi-free Oscillation Measurements (Table 4)

It was desired to study the free oscillation of the GEM in roll and lateral displacement, but applying constraint to prevent fore-and-aft or vertical motion and yaw, and thus also providing a means for the accurate recording of the roll angle and the lateral displacement.

This was achieved by suspending the GEM in the long trapeze frame, the frame being pivoted parallel to the GEM roll axis 147.3cm above the surface board, and displacement of the frame relative to the vertical axis being recorded by a computer type low friction potentiometer attached to the main structure, the output being recorded on a Minneapolis-Honeywell Visicorder.

The GEM itself was also free to roll relative to the frame, and the vertical position of the roll pivots could be varied without altering the hover height of the GEM. The roll displacement relative to the trapeze was measured with an electrolytic potentiometer (thus ensuring no measurable constraint of the GEM roll motion), and recorded on the Visicorder.

Note that in the setup the GEM is not necessarily hovering and thus can be tested at greater altitudes than the engine power will support.

Great care was taken to minimize the inertia and stability effects of the trapeze frame.

#### 3.5(a) Measurement of Roll Damping

The GEM was supported in the trapeze frame with the pivot axis just above the CG, and the trapeze was locked to the ground board to prevent lateral motion.

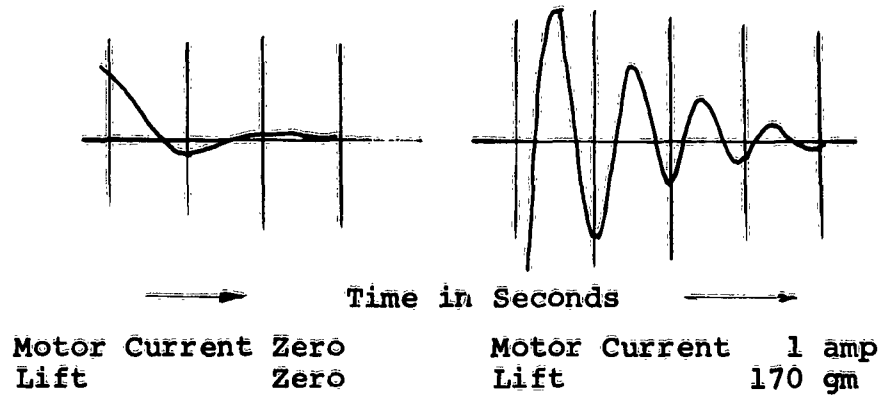
A typical oscillation is shown in Figure 17a for a ground clearance of 0.67cm ( $h/a = 0.032$ ). The frequency of oscillation and the damping factor are given in Table 4, corrected to the free flying weight of 288 grams.

#### 3.5(b) Measurement of Lateral Force Damping

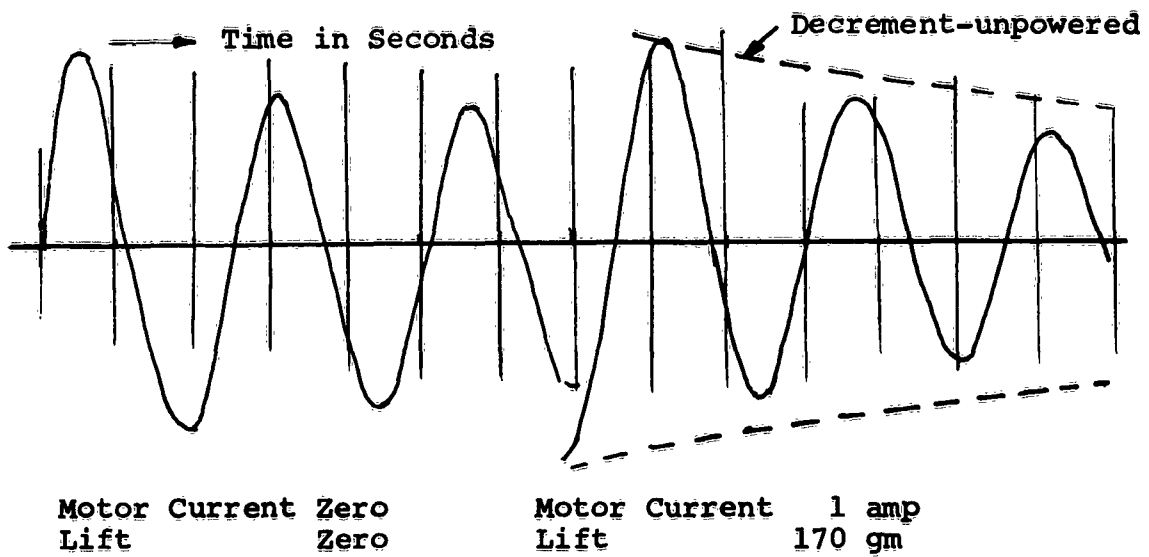
For this experiment the roll pivot was locked and the trapeze allowed to swing about the upper pivot assembly.

TABLE 4  
RESULTS OF OSCILLATION TESTS

Conditions of Test	Weight of model GEM Motor Current Lift exerted by GEM Rise Height	grams amperes grams cm.	288.6 1.0 or 0 170.0 or 0 0.66
Quantity	Symbol	Units	Observed Value
Nondimensional Stiffness in Roll	$\bar{M}_\phi$	-	0.982 0.97 in static tests of Section 3.3
Angular Displacement of Lift Vector relative to GEM, per radian of roll angle	$x_\phi$	-	-0.105 -0.03 in static tests of Section 3.4
Angular Frequency of Oscillation	$\omega$	radians per second	9.8 about fixed axis 10.1 about natural axis (interpolated)
Rolling Moment due to Rate of Roll	$M_\phi$	dyne centimeters per radian per second (gram cm./sec)	-96,700
Sideways Force Sideways Velocity	$D_x$	dynes per centimeter per second (grams/sec)	-23.7 power off -69.8 power on



(a) Roll Oscillation - Axis Fixed at Pivot 1



(b) Translational Oscillation - Roll Pivot Clamped

Figure 17. Roll and Translational Oscillations

Oscillations were recorded with and without the GEM power, thus from the difference of damping the damping force acting on the GEM due to lateral motion could be determined. Figure 17b.

Results are given in Table 4 for the GEM, corrected to a flying lift of 288 grams (since in the experiment the base lift was only 170 grams).

### 3.5(c) Determination of Effective Roll Axis for Free Flight

According to the simple theory of Section 2, a free-flying GEM tends to rotate in roll about an axis fixed in space above the CG, and provided that the constraint of the trapeze is negligible this can immediately be checked by free-flying both the roll axis and the trapeze axis, and allowing the GEM to oscillate in roll.

If oscillations are recorded about a series of roll pivot positions, varying from the lowest (below the CG) to the highest (well above the CG) then the lateral displacement oscillation should initially be in phase with the roll, gradually diminish to zero amplitude, and then increase in anti-phase with the roll oscillation. The effective roll axis is the point of zero excitation of the lateral oscillation, and according to the simple theory the distance of the axis above the CG is  $l_p = l_w$ , which equals  $l_e$ , the length of the simple equivalent pendulum, i.e., a simple pendulum with the same period as the GEM roll oscillation.

However, the trapeze does have some influence on the results, owing to its stability, its inertia, and to the fact that it can carry a portion of the weight of the GEM unless the lift is accurately equated to the weight. If the conditions at zero excitation are considered, however, the stability and inertia of the trapeze can be neglected, and care has been taken, in any case, to make these small, leaving only the effect of trapeze 'lift.'

If we assume that at the pivot a vertical force is exerted on the GEM equal to the difference between the weight  $W$  and the lift  $L$ , then it can easily be shown that the distance of the roll axis above the CG is now equal to  $l_e (L/W)$ .

Recordings were made of the two oscillations (roll and translational) with weights in the high and the low

positions, and with the pivots at stations (1) (low) and (6) (highest). The records for the high CG position were spoiled by eddy currents reflected from the walls of the room, but the low CG records were taken very quickly before the air currents formed, and seem reasonable. These are shown in Figures 18 and 19 and Table 4 gives the derived values of the parameters.

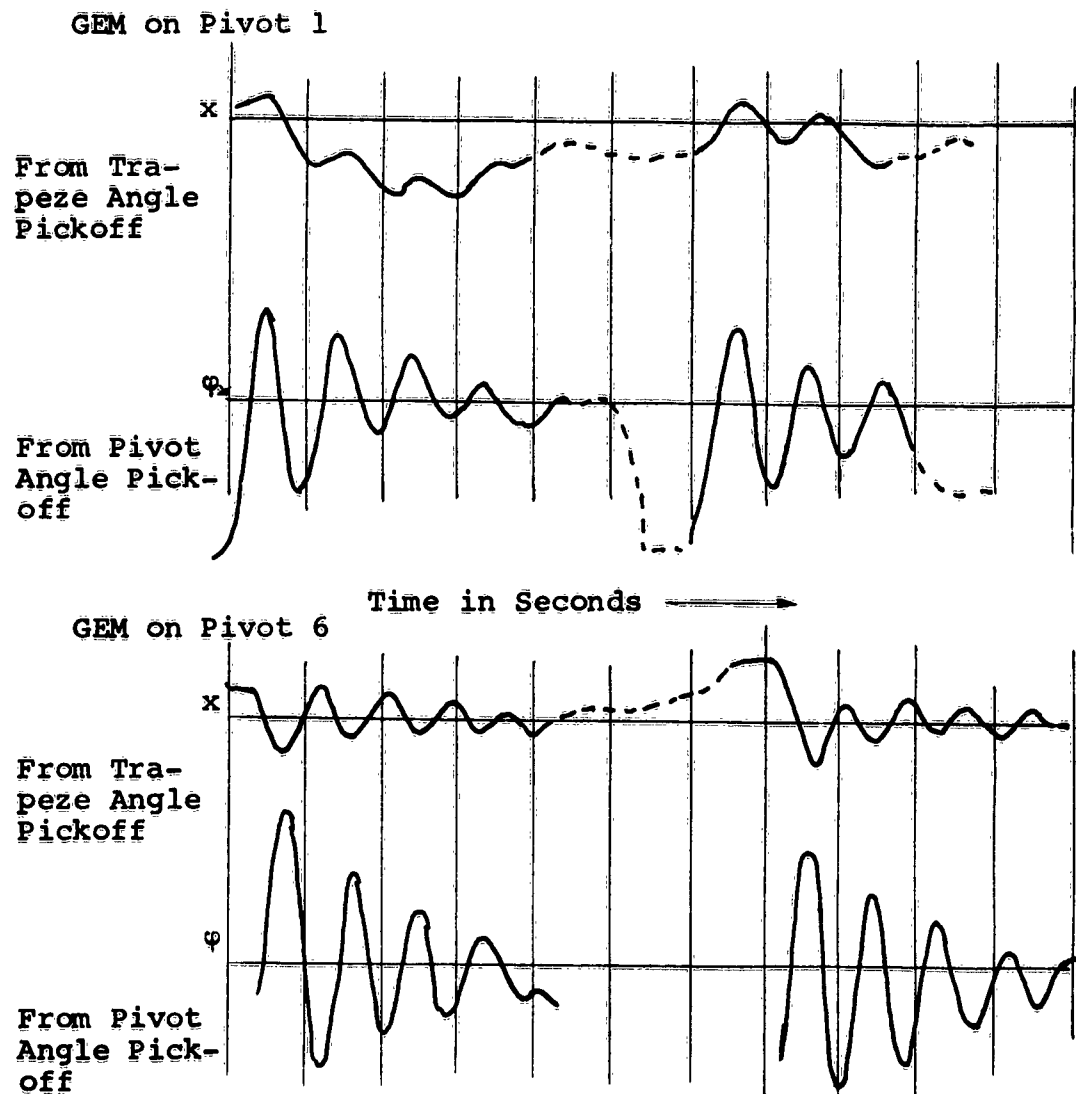


Figure 18. Coupled Oscillation (Low CG)

### 3.5(d) Stability About an Axis Located at the Base

Stanton-Jones' corrections for CG height lead to the conclusion that for the GEM to be stable in free flight, it must be stable about an axis at the base of the machine.

The GEM was therefore pivoted in roll at a height of 0.66cm. and the roll oscillations observed and filmed. It was found that the GEM was stable about this axis with a base lift of 288 grams and the CG in the low position, but was unstable with the CG in the high position. This behavior would be expected from the measured results of the static stability derivatives.

[To achieve this large lift it was necessary to replace the fans with fans of lower pitch to increase the efficiency of the air supply system and then to recalibrate the variation of altitude with input current. Figure 20.]

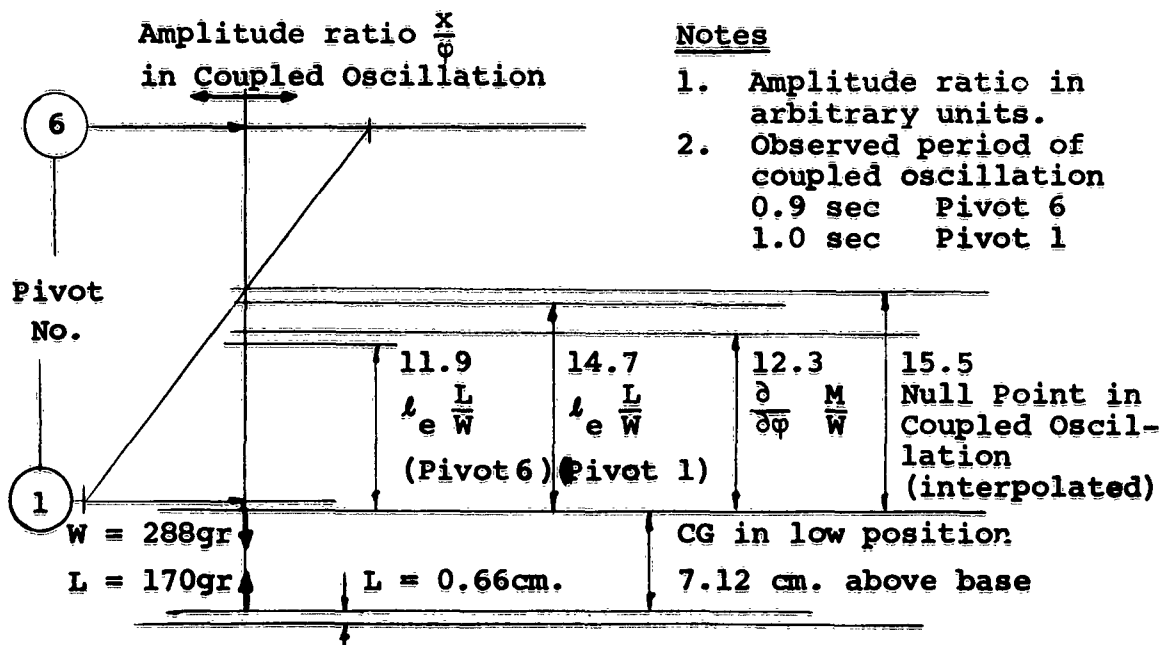


Figure 19. Determination of Roll Axis

### 3.6 Free Flight Measurements

The trapeze measurements of effective roll axis were insufficient to demonstrate conclusively the effects on stability of CG height, so as a final check free-flight tests were made.

Current was led to the GEM through a very flexible wire attached at the same height as the CG, but at one end of the machine. With this attachment it proved possible to control the machine position in yaw, and fore and aft, without exciting roll oscillations.

The roll oscillations were filmed, and the machine was found to be stable with either the high or the low CG, and the period was in good agreement with the calculated values based on the static derivatives.

It is therefore clear that stability about the base does not determine roll stability in free flight.

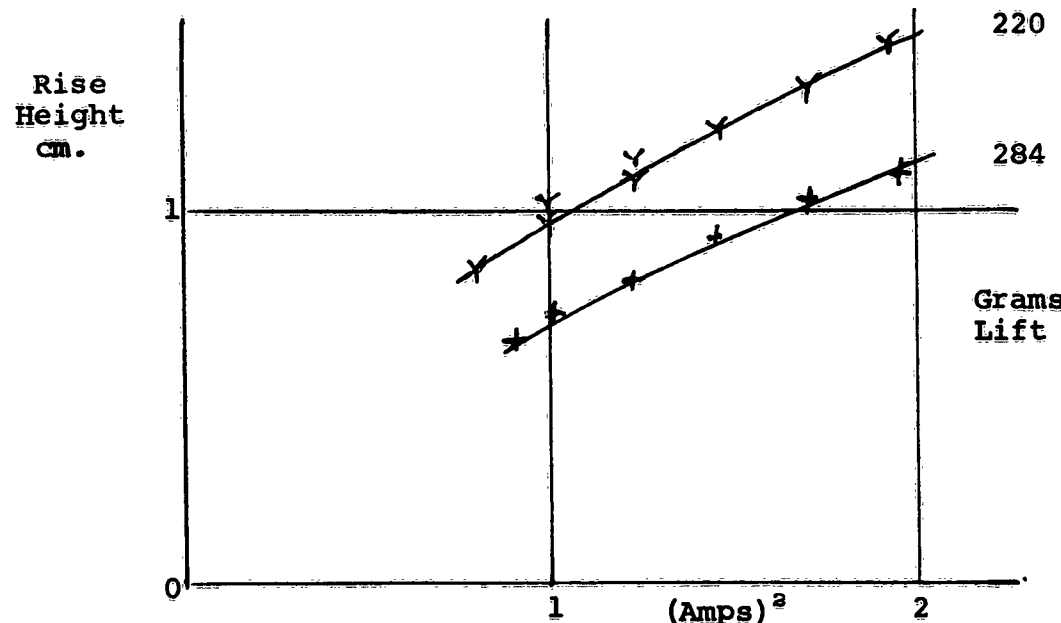


Figure 20. Variation of Rise Height with Current for Fixed Lifts Low Pitch Fans

#### 4. CONCLUSIONS

The theory and experiment described in the main body of this note show that

- a. The stability of the GEM in hover and not in contact with the ground or subject to large damping forces is determined by the moments about the center of gravity.
- b. The resultant lift acting on a "thin-jet" GEM is substantially normal to the base, and hence a variation of CG height has no effect on the stability of the GEM, as long as damping forces are small.
- c. If damping forces are very large, as when the GEM carries a keel which dips into the surface when flying over water, then to ensure stability the total moment about the point of application of the damping force must be stable. In these circumstances a high CG position is de-stabilizing.
- d. If a GEM with a flat base is flying over water at a low altitude, intermittent wave-top contacts may produce sufficient damping force to affect stability. In this case it may be appropriate to take moments about the base to determine the stability.

The full theory is developed in Appendix I and should be used whenever the damping forces are appreciable, but not dominant. The full theory shows:

- e. That the simple theory gives the correct results wherever the damping is low or dominant.
- f. In cases where the damping is appreciable, the simple definition of stability may be insufficient. A good guide may be the analysis of Appendix I, which determines the roll displacement due to sudden application of damping force, leading to contact with the surface.

In general it would seem that any practical CG position will be acceptable on stability grounds, and that there is no objection to the use of a high CG as recommended by Chaplin in reference 4 to improve dynamic stability at high speed.

REFERENCES

- 1 Stanton-Jones, R., Some Design Problems of Hovercraft, Institute of Aerospace Sciences Report 61-45.
- 2 Eames, M.C., Fundamental Principles of the Stability of Peripheral Jet Vehicles, PneumoDynamics Corp., Bethesda, Maryland.
- 3 Foltz, Claude A., Wind Tunnel Tests on a Series of Circular Ground Effect Machines, University of Wichita, Engineering Research Reports 352-1 through 352-7.
- 4 Chaplin, Harvey R., Design Study of a 29-Foot GEM, David Taylor Model Basin Report 1521.

## APPENDIX I

### FREE GEM EQUATIONS

#### INTRODUCTION AND SUMMARY

In the following analysis, equations describing the lateral and rolling motion of a free-flying GEM are derived, subject to the assumptions as stated. Three particular cases are then considered. In the first the GEM is acted on only by its weight and the lift and moment exerted by the base, and the motion following a rotational disturbance is examined. The effect of CG height on stability is briefly discussed. The second case introduces a side-ways force at the base such as might be generated by grazing contact with the ground or water surface. In the third case contact with the ground or other obstacle is such that the GEM is arrested at the point of contact. The subsequent angular excursion of the GEM is expressed as a function of the initial lateral velocity.

#### ASSUMPTIONS AND GENERAL CASE

1. Angles of rotation are small.
2. The weight  $W = mg$  is balanced by the lift  $L$ .
3. When the GEM rotates about its center of gravity through an angle  $\varphi$  the effective point of action of the lift  $L$  is displaced a distance  $p_a$  along the base, where  $a$  is the beam dimension and  $p$  is a linear function of  $\varphi$ . That is,  $p = p_\varphi \varphi$ . Further, the lift vector rotates relative to the GEM through an angle  $x$ , a linear function of  $\varphi$ , so that  $x = x_\varphi \varphi$ .
4. The drag  $D$  and the surface force  $F$  are both linear functions of the velocity of that point of the GEM at which they act.

That is,  $D = D$  times velocity at point of action of  $D$  and . .  $F = F$  times velocity at point of action of  $F$ .

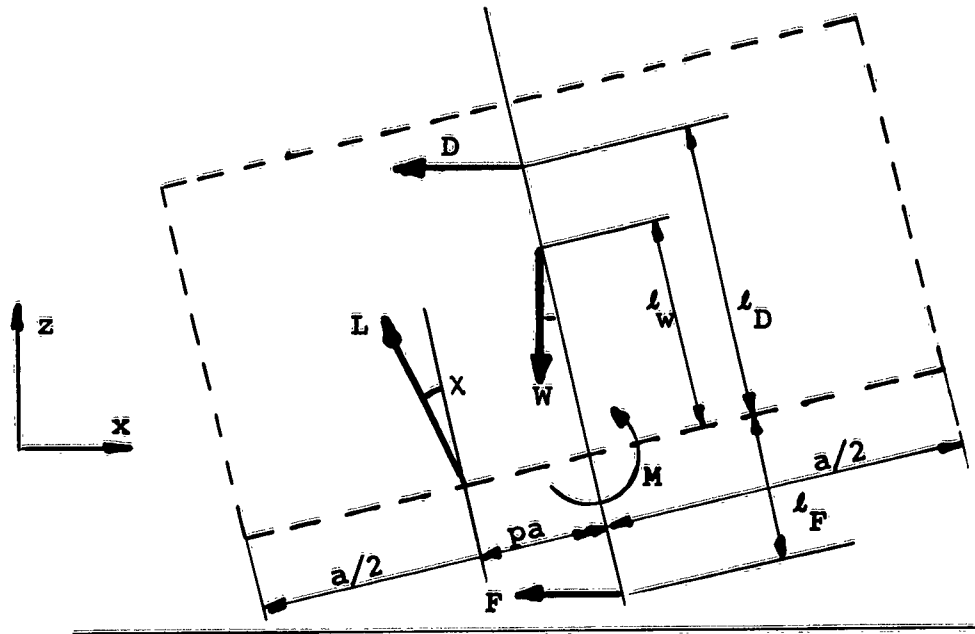


Figure 21. Rolling GEM - Notation used in Appendix I

Take space axes, and let CG be at  $(x, z)$ .

Resolving vertically:

$$L = W \quad (= mg) \quad (1)$$

Resolving horizontally:

$$m\ddot{x} = -L(\varphi + \dot{x}) - D - F$$

$$\text{i.e. } m\ddot{x} = -L(1+x_\varphi)\varphi - D_v\{\dot{x} - (l_D - l_W)\dot{\varphi}\} - F_v\{\dot{x} + (l_W + l_F)\dot{\varphi}\}$$

$$\text{i.e. } m\ddot{x} + (D_v + F_v)\dot{x} = \{D_v(l_D - l_W) - F_v(l_W + l_F)\}\dot{\varphi} = L(1+x_\varphi)\varphi \quad (2)$$

Taking moments about G:

$$I\ddot{\phi} = -L(ap + \ell_w x) + D_v (\ell_D - \ell_w) \{\dot{x} - (\ell_D - \ell_w) \dot{\phi}\} \\ - F_v (\ell_w + \ell_F) \{\dot{x} + (\ell_w + \ell_F) \dot{\phi}\} - M_x \dot{\phi}$$

where  $M_x \dot{\phi}$  is the angular damping.

$$\text{i.e. } I\ddot{\phi} + \{D_v (\ell_D - \ell_w)^2 + F_v (\ell_w + \ell_F)^2 + M_x\} \dot{\phi} + L(ap\dot{\phi} + \ell_w x\dot{\phi}) \dot{\phi} \\ = \{D_v (\ell_D - \ell_w) - F_v (\ell_w + \ell_F)\} \dot{x} \quad (3)$$

#### CASE WHEN D AND F ARE BOTH ZERO

Then the equations (2) and (3) become:

$$\ddot{x} = -g(1 + x_\phi) \dot{\phi} \quad (4)$$

and

$$\ddot{\phi} + \frac{M_x}{I} \dot{\phi} + \frac{mg}{I} (ap_\phi + \ell_w x_\phi) \dot{\phi} = 0 \quad (5)$$

Equation (5) can be written in the form

$$\ddot{\phi} + 2\zeta\omega_n \dot{\phi} + \omega_n^2 \phi = 0 \quad (6)$$

and is representative, under stable conditions, of a damped simple harmonic motion of natural rotational frequency  $\omega_n$  and damping factor  $\zeta$ .

The solution is of form:

$$\varphi = \varphi_0 e^{-\alpha t} \cos \omega t \quad (7)$$

whence

$$\alpha = \zeta \omega_n \quad (8)$$

also

$$\omega^2 = \omega_n^2 (1 - \zeta^2) \quad (9)$$

and

$$\omega_n^2 = \frac{mg}{I} (ap_\varphi + l_w x_\varphi) \quad (10)$$

and

$$\zeta = \frac{\frac{M_r}{I}}{2\sqrt{mgI(ap_\varphi + l_w x_\varphi)}} = \frac{M_r}{2\omega_n I} \quad (11)$$

Now equation (4) indicates an oscillatory motion in the x direction, since the driving function  $\varphi$  is oscillatory. The frequencies will be the same, but there may be a phase difference between the motions.

Assume that x is of form:

$$x = x_0 e^{-\alpha t} \cos (\omega t + \gamma) \quad (12)$$

Substituting this in equation (4) together with the solution for  $\varphi$  yields:

$$x_0 = -\varphi_0 \frac{I}{m} \frac{(1 + x_\varphi)}{(ap_\varphi + l_w x_\varphi)} \quad (13)$$

$$\tan \gamma = \frac{2\alpha\omega}{\alpha^2 - \omega^2} = \frac{2\zeta\sqrt{1-\zeta^2}}{2\zeta^2 - 1} \quad (14)$$

$$\sin \gamma = \frac{2\alpha\omega}{\alpha^2 + \omega^2} = 2\zeta\sqrt{1-\zeta^2} \quad (15)$$

$$\cos \gamma = \frac{\alpha^2 - \omega^2}{\alpha^2 + \omega^2} = 2\zeta^2 - 1 \quad (16)$$

Thus the solutions to the equations of motion are:

$$\left. \begin{aligned} \phi &= \phi_0 e^{-\alpha t} \cos \omega t \\ \text{and} \\ x &= -\phi_0 \frac{I}{m} \cdot \frac{(1 + x_\phi)}{(I_{ap\phi} + I_w x_\phi)} \cdot e^{-\alpha t} \cos (\omega t + \gamma) \end{aligned} \right\} \quad (17)$$

where  $w$  is given by equation (9),  $\gamma$  is given in terms of  $\zeta$  by equations (14), (15) and (16), and  $\zeta$  is given by equation (11).

#### The Effective Point of Rotation

Consider the point where the GEM axis extended intersects the z-axis.

The intercept on the GEM axis from this point to the CG is approximately  $\frac{x}{\phi}$

$$\text{i.e. } -\frac{I}{m} \cdot \frac{(1 + x_\phi)}{(I_{ap\phi} + I_w x_\phi)} \cdot \frac{\cos(\omega t + \gamma)}{\cos \omega t} \quad (18)$$

This is the length of the effective pendulum, and is invariant except for the effect of the phase angle  $\gamma$ , i.e., of the damping  $\zeta$ .

### The Effect of CG Height on Stability

$$\zeta = \frac{M_r}{2\sqrt{mgI}(ap_\varphi + l_w x_\varphi)} \quad \text{from equation (11)}$$

$\zeta$  will be  $> 0$  provided that  $M_r < 0$

and

$$(ap_\varphi + l_w x_\varphi) < 0$$

$p_\varphi$  and  $x_\varphi$  are determined by the configuration of the base of the GEM.

In the present model  $p_\varphi < 0$ ,  $x_\varphi < 0$ ,  $M_r < 0$  so that an increase in CG height ( $l_w$ ) decreases stability. In general, provided that the GEM is stable:

- if  $p_\varphi$  and  $x_\varphi$  both  $< 0$ , increase in  $l_w$  decreases stability.
- if  $p_\varphi$  and  $x_\varphi$  both  $> 0$ , increase in  $l_w$  increases stability.
- if  $p_\varphi < 0$  but  $x_\varphi > 0$ , increase in  $l_w$  increases stability.

### CASE WHEN F IS NOT ZERO

When F and L predominate, equations (2) and (3) become:

$$m\ddot{x} + F_v \dot{x} = -F_v(l_w + l_F)\dot{\varphi} - L(1 + x_\varphi)\varphi \quad (19)$$

$$I\ddot{\varphi} + F_v(l_w + l_F)^2 \dot{\varphi} + L(ap_\varphi + l_w x_\varphi)\varphi = -F_v(l_w + l_F) \dot{x} \quad (20)$$

[ $M_r$  is neglected in comparison with  $F_v(l_w + l_F)^2$ ].

Taking Laplace Transforms, and eliminating  $x$  terms results, after simplification, in:

$$\left[ p^3 + \left\{ \frac{F_v}{I} (\ell_w + \ell_F)^2 + \frac{F_v}{m} \right\} p^2 + \frac{L}{I} (ap_\varphi + \ell_w x_\varphi) p + \frac{F_v L}{mI} \left\{ (ap_\varphi - \ell_F x_\varphi) - (\ell_w + \ell_F) \right\} \right] \bar{\varphi} = \frac{F_v}{I} (\ell_w + \ell_F) U \quad (21)$$

where  $\dot{x} = -U$  when  $t = 0$ .

Now a cubic equation for a stable system indicates a subsidence and a damped oscillation, and is of form:

$$(p + \alpha)(p^2 + 2\zeta\omega_n\varphi + \omega_n^2) \bar{\varphi} = kU \quad (22)$$

Under the conditions selected  $\zeta$  will be small by comparison with  $\alpha$  and  $\omega_n$ . Thus equation (22) may be re-written:

$$\left[ p^3 + \alpha p^2 + \omega_n^2 p + \alpha \omega_n^2 \right] \bar{\varphi} = kU \quad (23)$$

Comparing coefficients of equations (21) and (23) gives:

$$\alpha = F_v \left\{ \frac{(\ell_w + \ell_F)^2}{I} + \frac{1}{m} \right\} \quad (24)$$

$$\omega_n^2 = \frac{L}{I} (ap_\varphi + \ell_w x_\varphi) \quad (25)$$

$$\alpha \omega_n^2 = \frac{F_v L}{mI} \left\{ (ap_\varphi - \ell_F x_\varphi) - (\ell_w + \ell_F) \right\} \quad (26)$$

If the assumptions regarding the relative magnitudes of  $\zeta$ ,  $\alpha$  and  $\omega_n$  are justified, then the above equations should be consistent,

i.e. (24) x (25) = (26), which leads to:

$$\frac{L(ap_\varphi - \ell_F x_\varphi)}{I + m(\ell_w + \ell_F)^2} - \frac{mg(\ell_w + \ell_F)}{I + m(\ell_w + \ell_F)^2} = \frac{L(ap_\varphi + \ell_w x_\varphi)}{I} \quad (27)$$

The left-hand side of the equation is the square of the angular rotational frequency of the system about the surface point. The right-hand side represents the similar parameter for rotation about the CG. Thus the assumptions made imply that the system would behave similarly when pivoted about the surface point as when pivoted about the CG.

#### OSCILLATION ABOUT SURFACE POINT OF CONTACT

In the event that in the course of translational motion a central keel or other projection should strike the surface, the GEM will tend to rotate about this point.

If the forward lower extremity of the vehicle is to avoid also striking the surface, the maximum permissible angular rotation is:

$$\varphi_{\max} = \frac{h}{a/2}$$

Taking moments about the surface point, which is considered as fixed, leads to:

$$\ddot{\varphi} + \frac{M_r}{I_p} \dot{\varphi} + \frac{\{L(ap_{\varphi} - l_F x_{\varphi}) - W(l_w + l_F)\} \varphi}{I_p} = 0 \quad (28)$$

where

$$I_p = I + m (l_w + l_F)^2 \text{ and } L = W = mg$$

and when

$$t = 0, \varphi = \varphi_0 = \frac{U}{l_F} \quad (\text{i.e. initial lateral velocity of base } U.)$$

Compare (28) with:

$$\ddot{\varphi} + 2\zeta \Omega_n \dot{\varphi} + \Omega_n^2 \varphi = 0 \quad (29)$$

The solution to equation (29) is:

$$\dot{\phi} = \frac{\dot{\phi}_0}{\Omega} e^{-\Omega t} \sin \Omega t \quad (30)$$

and the maximum value of  $\dot{\phi}$  is:

$$\dot{\phi}_{\max} = \frac{\dot{\phi}_0}{\Omega} e^{-\frac{\pi \alpha}{2\Omega}} \approx \frac{U}{\Omega n L_p} \quad (31)$$

where

$$\Omega_n^2 = \frac{W}{L_p} \{ a p_{\phi} - I_w - I_p (1 + x_{\phi}) \} \quad (32)$$

## APPENDIX II

### COLLECTED DATA ON THE ROTATION OF THE RESULTANT FORCE VECTOR WITH GEM ROTATION

#### INTRODUCTION

It would seem obvious at first sight that the resultant force on a GEM would always be normal at the base, independent of the roll or pitch angle, since the major part of the resultant force is due to the pressure at the base.

However, in the case of the plenum chamber, Ken Wernicke of Bell Aircraft has shown that the resultant force rotates faster than the normal, and in the limit, twice as fast.

The following information was collected from all available wind tunnel data in the attempt to show whether or not the results for thick jet GEMs tend toward the plenum chamber result as other GEM properties do.

#### RESULTS

##### University of Wichita Tests

The University of Wichita, Engineering Research Division have concluded a long series of generalized wind tunnel tests on ground effect machines, but the results of most tests are not sufficiently accurate to check the angle of lift because the internal aerodynamics of the model (which was supplied with air from an external source) evidently varied as the model incidence was changed.

The writer had one additional series of tests run, the "slanted ground board tests" in which the models were held at all times at zero incidence to the tunnel, but the ground board incidence was changed. This test therefore gives the static lift and drag acting on the model on model axes. Tests were run at  $+2.5^\circ$  and  $-2.5^\circ$  ground board setting and it may be assumed that any difference in model drag will be due to rotation of the resultant force vector (assuming that the flow distribution in the jet is not affected by the incidence in such a way as to give a drag force on body axes. This seems plausible, at least when  $\lambda$ , the jet-inclination angle, is small.)

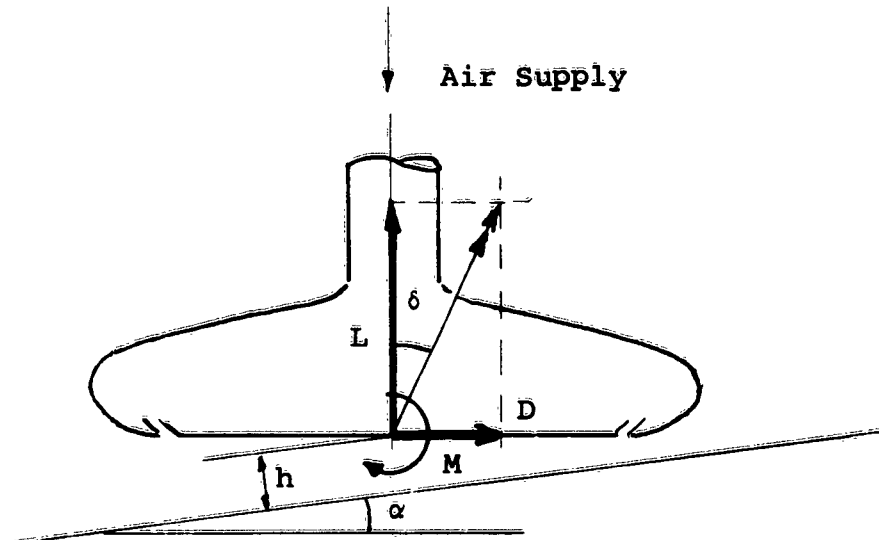


Figure 22. Force Diagram of Wichita Tests

Figure 22 shows the force diagram for the Wichita tests, with the ground board set at incidence as explained.

$$\tan \delta = \frac{D}{L}$$

In practice,

$$\tan \delta = \frac{D(\alpha = + 2.5 \text{ deg}) - D(\alpha = - 2.5 \text{ deg})}{L(\alpha = + 2.5 \text{ deg}) - L(\alpha = - 2.5 \text{ deg})}$$

because the value of D at  $\alpha = 0$  was appreciable owing to reactions of the supply pipe to the air supply.

If Wernicke's theory holds,

$$\frac{\tan \delta}{\tan \alpha} \rightarrow + 1.0 \text{ as } \frac{G}{h} \rightarrow \infty$$

If the resultant force is normal to the base

$$\frac{\tan \delta}{\tan \alpha} = 0$$

TABLE 5  
TYPICAL TABULATED RESULTS

Run	t/d	h/d	L	D	$\lambda = 0^\circ$		$h/G_e$	$\alpha$	$\frac{\tan \delta}{\tan \alpha}$	$\tilde{M}_p$	Symbol
					M	$G_e/d$					
2710	10%	3%	35.8	+	.772	2.60	.090	.33	+2.5°	.625	- .33
2715	10%	3%	34.6	-	1.145	1.23			-2.5°		○
2711	10%	5%	14.16	-	.548	4.02	:090	:56	+2.5°	.59	- .78
2714	10%	5%	14.87	-	.199	2.90			-2.5°		○
2712	10%	10%	5.08	-	.050	.20	.090	1.11	+2.5°	.29	+ .13
2713	10%	10%	4.75	-	.075	.27			-2.5°		○
2745	5%	3%	47.9	2.091	10.40		.0475.	.63	+2.5°	.12	-1.76
2740	5%	3%	43.1	1.619	1.085				-2.5°		○
2744	5%	5%	31.9	1.619	3.13		.0475	1.05	+2.5°	.10	- .42
2741	5%	5%	30.7	1.345	1.60				-2.5°		○
2743	5%	10%	17.90	1.370	6.94		.0475	2.10		-.03	- .02
2742	5%	10%	17.40	1.429	6.89						○
2758	1%	3%	36.01	.299	4.416		.0099	3	+2.5°	0	- .43
2763	1%	3%	36.51	.299	2.609				-2.5°		○
2759	1%	5%	24.48	.025	2.22		.0099	5	+2.5°	-.09	+ .53
2762	1%	5%	35.39	.174	3.75				-2.5°		○
2760	1%	10%	13.05	.075	1.48		.0099	10	+2.5°	-.07	+ .25
2761	1%	10%	10.22	0	1.81				-2.5°		○

Wichita Tests - UWER 352-5/supp. 9

Results are plotted in Figure 24 and at first sight show a strong tendency toward the Wernicke theory for

$$\frac{h}{G_e} < 1.5$$

In fact this conclusion may be erroneous. The only tests for which  $\tan \delta / \tan \alpha$  definitely exceeds 0 are  $h/d = 10\%$  and 5%,  $\lambda = 0^\circ$  and  $30^\circ$ , for which the jet flow distribution is very poor and conditions inside the model may in any case approach the plenum.

NASA Tests (reported in NASA Tech. Note D.317)

NASA tested a thin circular GEM with external air supply. Incidence was varied by rotation of the model about the supply pipes thus minimizing effects due to air flow.

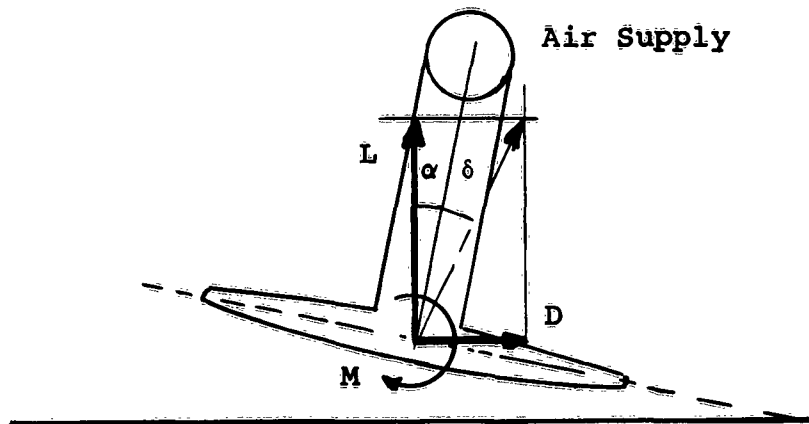


Figure 23. Force Diagram for NASA Tests

Lift and drag were measured on a wind tunnel balance, and designated  $T_y$ ,  $T_H$  in TN D317.

Here,  $\tan(\alpha + \delta) = \frac{L}{D}$   
 $\tan \delta = \frac{L}{D}$   
 $\frac{\tan \delta}{\tan \alpha} \frac{\tan \alpha}{\tan \delta} = 1$

for small values of  $\delta$

TABLE 6  
RESULTS OF NASA TESTS

		$\frac{h}{d} = 0.05$			$\frac{h}{d} = 0.11$		
$\alpha$	$\tan \alpha$	L	D	$\frac{D}{L}$	L	D	$\frac{D}{L}$
-8	-.140	----	----	----	1.10	.185	.168
-4	-.070	2.04	-.145	-.071	1.33	.110	.083
-2	-.035	2.30	-.055	-.028	----	----	----
0	0	2.50	+.03	+.012	1.50	0	0
2	+.035	2.42	.120	.050	----	----	----
4	.070	2.22	.200	.091	1.52	-.12	.079
8	.140	----	----	----	1.32	-.21	.159

Cross plotting these results gives

$$h/G_e = 8.6$$

$$\frac{\tan \delta}{\tan \alpha} = 0.115$$

$$h/G_e = 19.0$$

$$\frac{\tan \delta}{\tan \alpha} = -0.116$$

These results are plotted on Figure 24 and agree with the Wichita data.

English Electric Company

Mr. Roland Hunt has data on one thick jet condition,  $t/d = 0.10$  near the ground. Results are being sent from England and apparently agree with the trend towards the plenum. Figure 24. [These results have now been plotted :

$$\alpha = \pm 2.5^\circ \quad \frac{h}{G_e} = 1.05 \quad \frac{\tan \delta}{\tan \alpha} = 0.221. \quad \lambda = 0^\circ$$

agreeing with Wichita.

But for

$$\alpha = \pm 10^\circ, \frac{\tan \delta}{\tan \alpha} \text{ is increased to 0.45}.$$

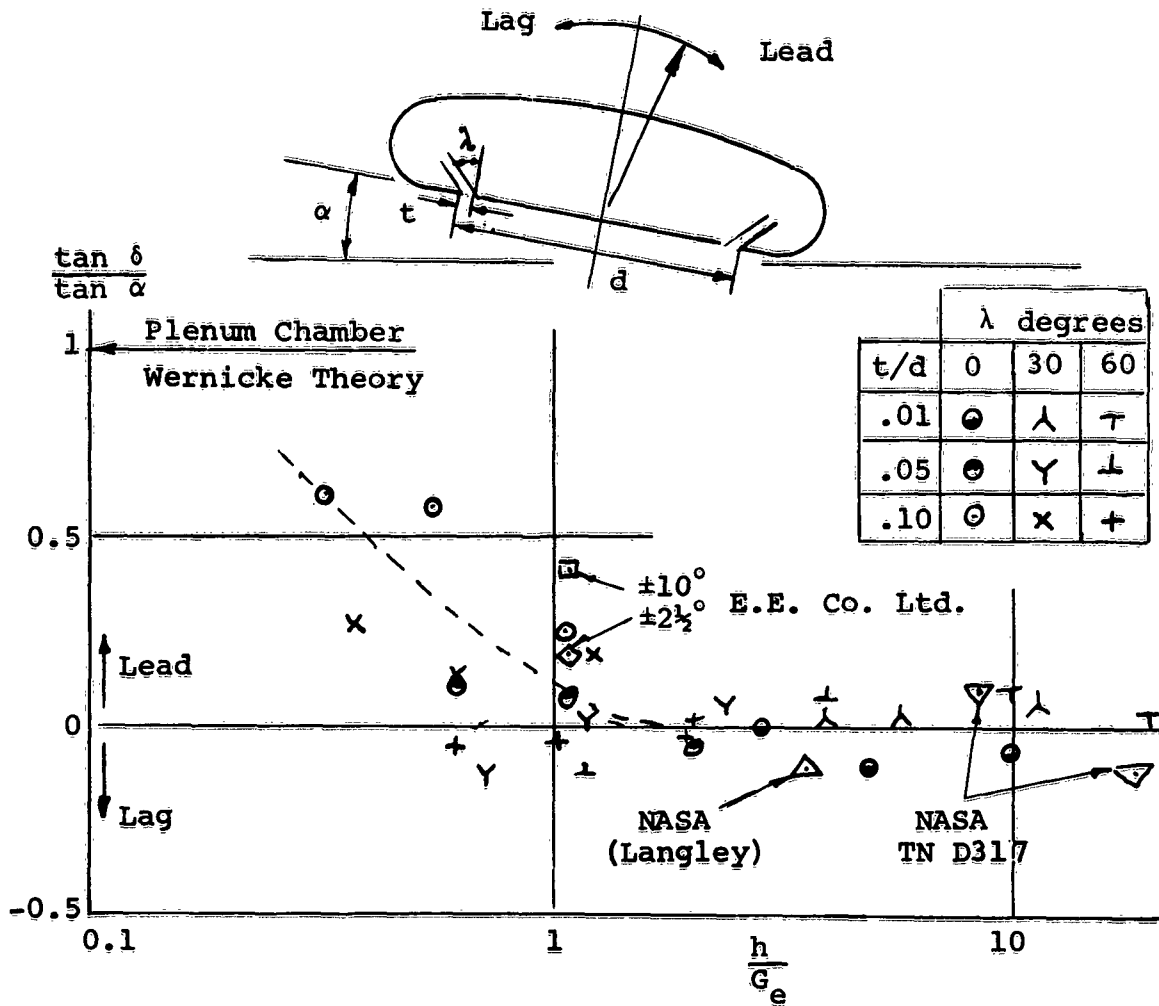


Figure 24. Collected Results (Appendix II)

### CONCLUSIONS

For the usual run of thin jet designs  $G_e < \frac{h}{2}$  and all evidence agrees that in such cases the resultant force is substantially normal to the base

$$\text{i.e. } \frac{\tan \delta}{\tan \alpha} = -0.1 \text{ to } + 0.1.$$

There will probably be a tendency with thick jet machines operating at low altitude for results to tend to the Wernicke theory as  $h/G_e \rightarrow 0.2$ . This implies that the resultant force vector leads the normal, and that the resulting restoring moments will be greater the higher the CG position.

DISTRIBUTION

USAWC	1
USATMC(FTZAT), ATO	1
USAPRDC	1
DCSLOG	1
Rsch Anal Corp	1
ARO Durham	2
OCRD, DA	2
NATC	1
ARO, OCRD	1
DCSOPS	1
USAERDL	2
USATAC, Center Line	4
OrdBd	1
CofT	3
USATCDA	1
USATMC	19
USATSCH	4
USATRECOM	73
TCLO, USAABELCTBD	1
USATRECOM LO, USARDG (EUR)	3
CNO	1
CNR	3
BUWEPS, DN	2
ACRD(OW), DN	1
USNSRDF	1
USNPGSCH	1
BUSHP, DN	1
USNOTS	1
Dav Tay Mod Bas	1
MCLFDC	1
MCEC	1
USASGCA	1
Canadian LO, USATSCH	3
BRAS, DAQMG(Mov & Tn)	4
USASG, UK	1
Langley Rsch Cen, NASA	2
NASA, Wash., D. C.	6
Ames Rsch Cen, NASA	2
Lewis Rsch Cen, NASA	1
USGPO	1

ASTIA	10
USAMRDC	1
HUMRRO	2
DDRE	1
US Mar Adm	1
HUMEL	1
MOCOM	3
AMC	1
Norman K. Walker Assoc., Inc.	10

<p>1. stability Inc., Bethesda, Maryland, THE EFFECT OF THE VERTICAL POSITION OF THE CENTER OF GRAVITY ON THE STABILITY OF AN ANNULAR JET GROUND EFFECT MACHINE - N. K. Walker and A. Anthony, TCREC Technical Rept 62-101, Dec. 1962, 54 pp. incl. illus. and tables (Contract DA 44-177-TC- 830) USATRECOM Task 9R99-01- 005-02.</p>	<p>1. stability Inc., Bethesda, Maryland, THE EFFECT OF THE VERTICAL POSITION OF THE CENTER OF GRAVITY ON THE STABILITY OF AN ANNULAR JET GROUND EFFECT MACHINE - N. K. Walker and A. Anthony, TCREC Technical Rept 62-101, Dec. 1962, 54 pp. incl. illus. and tables (Contract DA 44-177-TC- 830) USATRECOM Task 9R99-01- 005-02.</p>	<p>1. stability Inc., Bethesda, Maryland, THE EFFECT OF THE VERTICAL POSITION OF THE CENTER OF GRAVITY ON THE STABILITY OF AN ANNULAR JET GROUND EFFECT MACHINE - N. K. Walker and A. Anthony, TCREC Technical Rept 62-101, Dec. 1962, 54 pp. incl. illus. and tables (Contract DA 44-177-TC- 830) USATRECOM Task 9R99-01- 005-02.</p>
<p>Unclassified Report Lift, sideforce and rolling (over)</p>	<p>Unclassified Report Lift, sideforce and rolling (over)</p>	<p>Unclassified Report Lift, sideforce and rolling (over)</p>

moment were measured on a powered model thin annular jet GEM hovering with the motion restricted to the transverse plane.

The lift vector is shown to remain nearly normal to the base when the machine is rolled and so the stability in roll is unaffected by the height of the CG relative to the base, as long as the machine is clear of any obstacle which could exert large lateral forces on it. As a practical check the machine was flown free with the CG in positions one third, two thirds and finally one whole beam above the base, without affecting the dynamical stability.

moment were measured on a powered model thin annular jet GEM hovering with the motion restricted to the transverse plane.

The lift vector is shown to remain nearly normal to the base when the machine is rolled and so the stability in roll is unaffected by the height of the CG relative to the base, as long as the machine is clear of any obstacle which could exert large lateral forces on it. As a practical check the machine was flown free with the CG in positions one third, two thirds and finally one whole beam above the base, without affecting the dynamical stability.

moment were measured on a powered model thin annular jet GEM hovering with the motion restricted to the transverse plane.

The lift vector is shown to remain nearly normal to the base when the machine is rolled and so the stability in roll is unaffected by the height of the CG relative to the base, as long as the machine is clear of any obstacle which could exert large lateral forces on it. As a practical check the machine was flown free with the CG in positions one third, two thirds and finally one whole beam above the base, without affecting the dynamical stability.

moment were measured on a powered model thin annular jet GEM hovering with the motion restricted to the transverse plane.

The lift vector is shown to remain nearly normal to the base when the machine is rolled and so the stability in roll is unaffected by the height of the CG relative to the base, as long as the machine is clear of any obstacle which could exert large lateral forces on it. As a practical check the machine was flown free with the CG in positions one third, two thirds and finally one whole beam above the base, without affecting the dynamical stability.

<p>1. Stability</p> <p>2. Aerodynamics</p>	<p>1. Stability</p> <p>2. Aerodynamics</p>
<p>Norman K. Walker Associates, Inc., Bethesda, Maryland, THE EFFECT OF THE VERTICAL POSITION OF THE CENTER OF GRAVITY ON THE STABILITY OF AN ANNULAR JET GROUND EFFECT MACHINE - N. K. Walker and A. Anthony, TCREC Technical Rept 62-101, Dec. 1962, 54 pp. incl. illus. and tables (Contract DA 44-177-TC-830) USATRECOM Task 9R99-01-005-02.</p>	<p>Norman K. Walker Associates, Inc., Bethesda, Maryland, THE EFFECT OF THE VERTICAL POSITION OF THE CENTER OF GRAVITY ON THE STABILITY OF AN ANNULAR JET GROUND EFFECT MACHINE - N. K. Walker and A. Anthony, TCREC Technical Rept 62-101, Dec. 1962, 54 pp. incl. illus. and tables (Contract DA 44-177-TC-830) USATRECOM Task 9R99-01-005-02.</p>
<p>Unclassified Report</p> <p>Lift, sideforce and rolling (over)</p>	
<p>1. Stability</p> <p>2. Aerodynamics</p>	<p>1. Stability</p> <p>2. Aerodynamics</p>
<p>Norman K. Walker Associates, Inc., Bethesda, Maryland, THE EFFECT OF THE VERTICAL POSITION OF THE CENTER OF GRAVITY ON THE STABILITY OF AN ANNULAR JET GROUND EFFECT MACHINE - N. K. Walker and A. Anthony, TCREC Technical Rept 62-101, Dec. 1962, 54 pp. incl. illus. and tables (Contract DA 44-177-TC-830) USATRECOM Task 9R99-01-005-02.</p>	<p>Norman K. Walker Associates, Inc., Bethesda, Maryland, THE EFFECT OF THE VERTICAL POSITION OF THE CENTER OF GRAVITY ON THE STABILITY OF AN ANNULAR JET GROUND EFFECT MACHINE - N. K. Walker and A. Anthony, TCREC Technical Rept 62-101, Dec. 1962, 54 pp. incl. illus. and tables (Contract DA 44-177-TC-830) USATRECOM Task 9R99-01-005-02.</p>
<p>Unclassified Report</p> <p>Lift, sideforce and rolling (over)</p>	

moment were measured on a powered model thin annular jet GEM hovering with the motion restricted to the transverse plane.

The lift vector is shown to remain nearly normal to the base when the machine is rolled and so the stability in roll is unaffected by the height of the CG relative to the base, as long as the machine is clear of any obstacle which could exert large lateral forces on it. As a practical check the machine was flown free with the CG in positions one third, two thirds and finally one whole beam above the base, without affecting the dynamical stability.

moment were measured on a powered model thin annular jet GEM hovering with the motion restricted to the transverse plane.

The lift vector is shown to remain nearly normal to the base when the machine is rolled and so the stability in roll is unaffected by the height of the CG relative to the base, as long as the machine is clear of any obstacle which could exert large lateral forces on it. As a practical check the machine was flown free with the CG in positions one third, two thirds and finally one whole beam above the base, without affecting the dynamical stability.

moment were measured on a powered model thin annular jet GEM hovering with the motion restricted to the transverse plane.

The lift vector is shown to remain nearly normal to the base when the machine is rolled and so the stability in roll is unaffected by the height of the CG relative to the base, as long as the machine is clear of any obstacle which could exert large lateral forces on it. As a practical check the machine was flown free with the CG in positions one third, two thirds and finally one whole beam above the base, without affecting the dynamical stability.

moment were measured on a powered model thin annular jet GEM hovering with the motion restricted to the transverse plane.

The lift vector is shown to remain nearly normal to the base when the machine is rolled and so the stability in roll is unaffected by the height of the CG relative to the base, as long as the machine is clear of any obstacle which could exert large lateral forces on it. As a practical check the machine was flown free with the CG in positions one third, two thirds and finally one whole beam above the base, without affecting the dynamical stability.